



U.S. DEPARTMENT OF THE INTERIOR  
U.S. GEOLOGICAL SURVEY

**GEOLOGIC MAP OF THE TETILLA PEAK QUADRANGLE,  
SANTA FE AND SANDOVAL COUNTIES, NEW MEXICO**

By

David A. Sawyer, Ralph R. Shroba, Scott A. Minor, and Ren A. Thompson

Digital compilation by Jeffrey C. Blossom, Thomas R. Fisher,  
Ronald R. Wahl, and D. Paco Van Sistine

2002

Pamphlet to accompany  
MISCELLANEOUS FIELD STUDIES MAP  
MF-2352

## DESCRIPTION OF MAP UNITS

### SURFICIAL DEPOSITS

Surficial deposits shown on the map are estimated to be at least 1 m thick. Most of the surficial deposits are poorly exposed. Thin, discontinuous sheetwash deposits on bedrock and small artificial fills were not mapped. Divisions of Pleistocene time are informal and are as follows: late Pleistocene 10,000–132,000 years, middle Pleistocene 132,000–788,000 years, and early Pleistocene 788,000 years to 1.81 million years (table 1; Lourens and others, 1996; Richmond and Fullerton, 1986). Age assignments for surficial deposits are based chiefly on the degree of modification of original surface morphology, height above modern perennial streams and arroyos, and degree of soil development. Some age assignments are based in part on work by Smith and Kuhle (1998) for similar or equivalent surficial deposits in the adjacent Santo Domingo quadrangle to the west. Soil-horizon designations are those of the Soil Survey Staff (1975), Guthrie and Witty (1982), and Birkeland (1999). Most of the surficial deposits are calcareous and contain different amounts of primary and secondary calcium carbonate; stages of secondary calcium carbonate morphology (referred to as stages I through III Bk or K soil horizons in this report) are those of Gile and others (1966). Grain sizes given for surficial deposits are based on field estimates and follow the modified Wentworth scale (American Geological Institute, 1982). In the descriptions of surficial deposits, the term “clasts” refers to the fraction greater than 2 mm in diameter, whereas the term “matrix” refers to the particles less than 2 mm in size. Dry matrix colors of the surficial deposits were determined by comparison with Munsell Soil Color Charts (Munsell Color, 1973). Colors of the surficial deposits correspond to those of the sediments and (or) bedrock from which they were derived. Surficial deposits commonly range from light gray (10YR 7/2) to light reddish brown (7.5YR 6/4). All of the map units that contain debris-flow deposits probably also contain hyperconcentrated-flow deposits, which are intermediate in character between stream-flow and debris-flow deposits. In this report, the term “alluvium” includes surficial materials transported by running water confined to channels (stream alluvium) as well as running water not confined to channels (sheetwash). The term “colluvium” includes surficial material transported down slopes by mass-wasting (gravity-driven) processes—such as creep and debris flow—aided by running water not confined to channels (sheetwash). Basaltic bedrock overlain by surficial deposits less than about 1 or 2 m thick is commonly mantled by a thin rubble that is well cemented by calcium carbonate with stage IV morphology. The divisions of geologic time used in this report are provided in table 1. Metric units are used in this report. A conversion table is provided for those more familiar with English units (table 2).

**Table 1.** Definitions of divisions of geologic time used in this report [After Hansen (1991) with exceptions (\*): 132,000 (late-middle Pleistocene) and 778,000 (middle-early Pleistocene) from David Fullerton (USGS, written commun., 1999); 1.81 million (Pleistocene-Pliocene) from Lourens and others (1996); 5.32 million (Pliocene-Miocene) from Berggren and others (1995b)]

| ERA      | Period     | Epoch         | Age (years)        |                       |
|----------|------------|---------------|--------------------|-----------------------|
| CENOZOIC | Quaternary | Holocene      | 0–10,000           |                       |
|          |            | Pleistocene   | late               | 10–132,000            |
|          |            |               | middle             | 132–778,000*          |
|          |            |               | early              | 778,000–1.81* million |
|          | Tertiary   | Pliocene      | 1.81–5.32* million |                       |
|          |            | Miocene       | 5.32–24 million    |                       |
|          |            | Oligocene     | 24–38 million      |                       |
|          | Eocene     | 38–55 million |                    |                       |
|          | Paleocene  | 55–66 million |                    |                       |
| MESOZOIC | Cretaceous |               | 66–138 million     |                       |
|          | Jurassic   |               | 38–205 million     |                       |
|          | Triassic   |               | 205–240 million    |                       |

**Table 2.** Factors for conversion of metric units to English units

| Multiply         | By     | To obtain |
|------------------|--------|-----------|
| centimeters (cm) | 0.3937 | inches    |
| meters (m)       | 3.2808 | feet      |
| kilometers (km)  | 0.6214 | miles     |

- af **Artificial fill deposits (latest Holocene)**—Uncompacted mine tailings and compacted fill material composed mainly of silt, sand, and rock fragments. Mapped chiefly beneath and near segments of Interstate 25 and along the Santa Fe River upstream of the mouth of Cañada de Santa Fe. Thickness generally less than 10 m
- Qal **Flood plain and stream channel deposits (Holocene and late(?) Pleistocene)**—Poorly sorted gravelly sand to clast-supported sandy gravel along the Santa Fe River and Galisteo Creek. Upper part of flood plain deposits may be finer grained than lower part. Low-lying areas of map unit are prone to periodic flooding. Unit Qal locally includes small deposits of undivided alluvium and colluvium (Qac), low terrace deposits less than 3 m above modern stream level, and sheetwash deposits (Qsw). Total thickness possibly 10–20 m
- Qac **Alluvium and colluvium, undivided (Holocene and late Pleistocene)**—Chiefly undifferentiated flood plain and stream channel deposits (Qal), sheetwash (Qsw), and minor fan alluvium and debris-flow deposits (Qfd) and debris-flow deposits (Qd). Unit Qac consists of silty sand to poorly sorted, clast- and matrix-supported, bouldery, cobbly pebble gravel with a sandy matrix. Pebbles and small cobbles are mainly of basaltic composition and a minor amount are of granitic and gneissic composition; large cobbles and boulders are of basaltic composition. Low-lying areas of unit Qac are prone to periodic flooding and debris-flow deposition. Deposits composed of well-sorted silty sand are prone to gullyng. Total thickness possibly about 5–20 m
- Qfd **Fan alluvium and debris-flow deposits (Holocene to middle(?) Pleistocene)**—Clast- and matrix-supported, bouldery, pebble-and-cobble gravel with a sandy matrix, and locally pebbly and cobbly slightly silty sand that contains gravel lenses. Pebbles and small cobbles are mainly of basaltic composition and a minor amount are of granitic and gneissic composition; large cobbles and boulders are of basaltic composition. Unit Qfd locally forms fan-shaped and lobate masses of sediment along the La Bajada escarpment, Santa Fe River, and the southern boundary of the map area. These masses of sediment were deposited by sediment-charged intermittent streams and debris flows. Low-lying areas of unit Qfd adjacent to stream channels are prone to periodic flooding and debris-flow deposition. Maximum thickness probably about 20 m
- Qf **Fan alluvium (Holocene to middle Pleistocene)**—Matrix-supported, pebbly and cobbly, slightly silty sand and minor deposits of clast- and matrix-supported, slightly bouldery, pebble-and-cobble gravel. Pebbles and small cobbles are mainly of basaltic composition and a minor amount are of granitic and gneissic composition; large cobbles and boulders are of basaltic composition. Unit Qf was deposited chiefly by intermittent streams and locally by debris flows along the La Bajada escarpment, Santa Fe River, and Cienega Creek. Unmapped sheetwash deposits (Qsw) are locally present and are lumped with Qf. Low-lying areas of unit Qf adjacent to stream channels are prone to periodic flooding and locally to debris-flow deposition. Maximum thickness probably about 30 m
- Qc **Colluvium, undivided (Holocene to middle(?) Pleistocene)**—Unit locally includes sheetwash (Qsw), debris-flow (Qd), landslide (Qls), talus (rock-fall), undivided alluvium and colluvium (Qac), and creep-deformed deposits that are too small to map separately or that lack distinctive surface morphology and could not be distinguished in the field or on aerial photographs. Deposits range in size from silty sand to bouldery basaltic rubble. Clasts are commonly of basaltic composition. Unit Qc is commonly present on the flanks of mesas below basaltic lava flows. Maximum thickness possibly about 30 m
- Qd **Debris-flow deposits (Holocene to middle(?) Pleistocene)**—Lobate and fan-shaped masses of debris deposited by sediment-charged flows at and near the base of the steep La Bajada escarpment and along the Santa Fe River and the southern boundary of the map area. Deposits are very poorly sorted and very poorly stratified boulders to granules supported in a sandy matrix. Lenticular beds of poorly sorted, clast-supported, bouldery, cobbly, pebble gravel with a sandy matrix are locally present. Clasts are commonly of basaltic composition and angular to subangular, and appear to be randomly oriented. Low-lying areas of unit Qd adjacent to stream channels are prone to periodic flooding and debris-flow deposition. Maximum thickness possibly about 15 m
- Qsw **Sheetwash deposits (Holocene to middle (?) Pleistocene)**—Slightly pebbly to pebbly and cobbly, quartz-rich, sand and silty sand that are probably derived chiefly from eolian material and scattered clasts from the underlying gently sloping basaltic lava flows. Sand-size fraction is mostly very fine to medium. Strong southwesterly winds may have blown sand from former sparsely vegetated or actively aggrading flood plain deposits along the Rio Grande to the Cerros del Rio volcanic field. Some of the silt- and clay-size fraction in unit Qsw may have been derived from more distant sources (Shroba and Thompson, 1998). Sand and basaltic clasts were redeposited chiefly by gravity-driven slope processes and by unchanneled surface flow. Unit Qsw locally contains rare fragments

of reworked Guaje(?) Pumice Bed of the Otowi Member of the Bandelier Tuff [1.61 Ma (million years); Izett and Obradovich (1994)] erupted from the nearby Valles Caldera; and locally includes small deposits of undivided alluvium and colluvium (**Qac**). Fragments and deposits of pumice of the El Cajete Member of the Valles Rhyolite [~60 ka (ka, thousand years) Reneau and others, 1996] and deposits of eolian sand may be locally present on or in unit **Qsw**, but were not observed. Small deposits of El Cajete pumice are locally present in the northwestern part of the adjacent Montoso Peak quadrangle to the north (R.A. Thompson and R.R. Shroba, USGS, unpub. mapping, 1998). Low-lying areas of unit **Qsw** are prone to periodic sheet and stream flooding and gullying. Presence of surface and buried soils formed in unit indicates periodic deposition followed by surface stability and soil development. Shallow stream and road cuts usually expose two deposits. Upper deposit is commonly about 1 m thick. Soil formed in upper deposit has a weak argillic (Bt) horizon, about 20 cm thick, that overlies an 80-cm-thick, calcic (Bk) horizon. The Bk horizon has stage I carbonate morphology in the upper half and from stage I to locally stage II morphology in the lower half. Lower deposit is similar in character to upper deposit and is greater than 1 m thick. The soil formed in the lower deposit has a calcic (K) horizon about 35 cm thick that has stage III morphology, and is locally overlain by an eroded argillic horizon about 10 cm thick. Soils data for northern and central New Mexico (Machette and others, 1997) suggest that upper deposit may be roughly about 10,000–20,000 years old and may have accumulated during or just prior to the Pinedale glaciation (about 12,000–35,000 years ago). Lower deposit may be about 35,000–75,000 years old and may predate the Pinedale glaciation. Maximum thickness possibly about 10 m

**Qls** **Landslide deposits (Holocene to early Pleistocene)**—Unsorted and unstratified rock debris and sediment commonly characterized by hummocky topography. Landslides commonly form on unstable slopes beneath lava flows that cap the steep-sided mesas in the map area. Slope failures probably initiate in sediments beneath the flows and propagate upward into the overlying flows. Some of the landslide deposits are locally bounded upslope by crescentic headwall scarps and downslope by lobate toes. Unit **Qls** includes debris-slide, debris-slump, and debris-flow deposits as defined by Varnes (1978). Sizes and lithologies of clasts and grain-size distributions of matrices of these deposits reflect those of the displaced bedrock units. Most clasts are of basaltic composition. Some of the older landslide deposits have thick soil K horizons with stage III carbonate morphology. Landslide deposits may be prone to continued movement or reactivation due to natural as well as human-induced processes. Unit **Qls** locally includes unmapped sheetwash (**Qsw**), creep-deformed colluvial deposits (**Qc**), and broken and displaced basaltic blocks west of the en-echelon west-stepping La Bajada fault zone. Lithology and stratigraphy of the most northern deposits of unit **Qls** correspond with those of the basalts and andesites of the Cerros del Rio volcanic field immediately adjacent to the east in the footwall of the La Bajada fault zone. The sequence of flows present east of the La Bajada fault zone was broken, offset, and transformed into a series of roughly north-trending, joint-bounded blocks that step down to the west. These blocks of basaltic bedrock were displaced and deformed by gravity-driven processes, possibly related to movement along the La Bajada fault zone. Landslide deposits include incipiently slid blocks in the La Bajada fault zone near the northwestern corner of the map area. These incipiently slid blocks may be offset by younger faults of the La Bajada fault zone, but no datums were observed in the landslide deposits. Maximum thickness possibly 300 m

**Qt** **Terrace alluvium (late and middle(?) Pleistocene)**—Stream alluvium that underlies eroded terrace remnants about 6, 12, 25, and 40 m above the Santa Fe River, about 25 m above Galisteo Creek, and about 6–12 m above unnamed streams tributary to the Santa Fe River. Along the Santa Fe River chiefly granitic, locally cobbly pebble gravel, pebble gravel, pebbly sand, and sand are poorly exposed. Clasts are commonly subangular and subrounded. Along Galisteo Creek chiefly moderately well sorted and thin-bedded (10–90 cm), clast-supported cobbly pebble gravel, matrix-supported sandy pebble gravel and pebbly sand, and sand. Very thin (1–7 cm) lenses of very fine sand, sandy silt, and clayey silt are locally present. Beds of trough cross-bedded pebble gravel are weakly cemented by calcium carbonate and locally form subtle ledges. Clasts in deposit along Galisteo Creek are commonly subangular and subrounded monzonite (?) porphyry, granite, and sandstone. Along unnamed streams tributary to the Santa Fe River, deposits consist of basalt-rich, pebbly sand to locally bouldery, cobbly pebble gravel. Clasts are angular to subangular and are as large as about 50 cm in intermediate diameter.

Sheetwash deposits (**Qsw**) locally mantle unit **Qt**. Base of unit **Qt** along the Santa Fe River and Galisteo Creek is not exposed and may be near or below the level of the adjacent flood plain and stream channel deposits (**Qal**). The 25-m terrace remnants along

the Santa Fe River and Galisteo Creek may be roughly equivalent in age to terraces at a similar height above stream level in the Española basin that have an estimated age of  $95 \pm 15$  ka (Dethier and McCoy, 1993). The 40-m terrace remnant along the Santa Fe River may be roughly equivalent in age to terraces at a similar height above stream level in the Española basin that have an estimated age of  $170 \pm 40$  ka (Dethier and McCoy, 1993). The 25-m and 40-m terrace remnants may be roughly equivalent in age to map units Qta<sub>4</sub> and Qtp<sub>4</sub> and Qta<sub>3</sub> and Qtp<sub>3</sub>, respectively, in the adjacent Santo Domingo quadrangle (Smith and Kuhle, 1998). Unit Qta<sub>4</sub> is overlain by eolian sand and silt, which contains the approximately 60-ka El Cajete pumice (Smith and Kuhle, 1998; Reneau and others, 1996). Exposed thickness 2–23 m; total thickness possibly 2–25 m

QTa

**Ancha Formation (late or middle Pleistocene to Pliocene)**—The Ancha Formation, as mapped and defined by Spiegel and Baldwin (1963, plate 3 and p. 45–50) in and near the map area, includes alluvial deposits of the ancestral Santa Fe River, distal alluvial-fan(?) deposits derived from the Sangre de Cristo Mountains, and ephemeral-stream and debris-flow deposits derived from Los Cerrillos (Cerrillos Hills). Some authors, such as Bachman and Mehnert (1978, p. 287), restricted the Ancha Formation to sediments below basaltic lava flows of the Cerros del Rio volcanic field. We follow the convention of Spiegel and Baldwin (1963) and map the Ancha Formation both above and below these flows (our map unit Tbs).

Deposits of the ancestral Santa Fe River consist of poorly sorted, clast-supported, slightly cobbly, pebble gravel, sandy pebble gravel, pebbly sand, and silty sand. Clasts are mostly granitic along with minor mafic metamorphic rocks, quartzite, and vein quartz. Cut-and-fill structures and trough crossbeds are locally present. Dense carbonate cements a 75- to 100-cm-thick zone about 50 cm above the base of the unit where the unit overlies impermeable or slightly permeable bedrock. Distal alluvial-fan(?) deposits derived from the Sangre de Cristo Mountains consist chiefly of silty sand and carbonate-cemented, granite-rich, pebbly sandstone. Ephemeral-stream and debris-flow deposits derived from Los Cerrillos are rich in monzonite porphyry. They commonly consist of poorly sorted, crudely stratified, clast-supported and locally matrix-supported, sandy, cobbly pebble gravel and pebble gravel, and poorly sorted, matrix-supported, pebbly and cobbly, slightly silty sand. Deposits above the basaltic lava flows locally contain thin discontinuous zones weakly cemented by calcium carbonate. Deposits below the basaltic lava flows contain numerous buried calcic (Bk and K) soil horizons with stage II and III carbonate morphology. These buried soil horizons indicate episodes of surface stability and soil development following episodic deposition. The calcium carbonate in these buried soils suggests semiarid climatic conditions during the late Pliocene, prior to the deposition of the overlying basalt flows (Tbs and Tbj). Unit QTa is similar in lithology and composition to the Santa Fe Group—eastern piedmont facies (Tsp), but differs from these sediments, which are displaced by east-dipping normal faults. Maximum thickness of deposits in unit QTa: ancestral Santa Fe River about 15 m; distal alluvial-fan(?) deposits derived from the Sangre de Cristo Mountains about 35 m; ephemeral-stream and debris-flow deposits derived from Los Cerrillos about 30 m above the lava flows and probably about 20 m below the lava flows

Qp

**Pediment deposits (middle Pleistocene)**—Mostly sandy alluvium on La Majada Mesa, west of the La Bajada fault zone, that overlies an extensive gently sloping (about 0.2–2 percent) erosion surface formed on upper Santa Fe Group sediments (QTs). This surface was graded to the Rio Grande and probably formed during a relatively long period of stability. Western limit of unit projects to about 75 m above the Rio Grande, about 7 km west of the map area. Unit Qp is very slightly silty sand that contains a minor amount of pebbles and cobbles. Clasts are chiefly of granitic and basaltic composition. Soil Bk horizons (about 45 cm thick) with stage II carbonate morphology and locally soil K horizons (about 10 cm thick) with stage III carbonate morphology are locally present in upper part of unit. Unmapped eolian sand or sheetwash deposits (Qsw) locally mantle top of unit. Unit Qp is equivalent to the alluvium of the La Majada Mesa surface of Smith and Kuhle (1998), who correlated the alluvium with the axial-terrace gravel of Dethier (1999), which is likely to be about 550–650 ka (Dethier and McCoy, 1993). Smith and Kuhle (1998) reported that the surface of the alluvium of the La Majada Mesa is commonly capped by a stage III to IV calcic soil horizon that is overlain by a stripped argillic B soil horizon. They also reported that the unit (locally?) contains numerous buried soils that suggest a complex history of alternating landscape stability and deposition. Unit Qp is similar in age or is slightly younger than the underlying “La Bajada pediment,” the intermediate surface of three high erosion surfaces graded to the Rio Grande (Bryan and McCann, 1938). Exposed thickness 2–6 m; maximum thickness possibly 10 or 15 m

**QTs**            **Upper Santa Fe Group sediments (middle or early Pleistocene to late(?) Pliocene)**—Slightly pebbly and cobbly, very slightly silty sand that contains lenses of pebbly and cobbly gravel. The gravel is rich in dark volcanic clasts and contains a minor amount of granitic clasts and vein quartz. Unit QTs was deposited west of the La Bajada fault zone and is poorly exposed below a depth of about 5 m. Available data suggest that unit QTs is younger than the underlying Pliocene basalt. Thickness, based on one drill hole (BIA well in cross section A–A' in Smith and Kuhle, 1998) just west of the map area in the Santo Domingo quadrangle (NW¼SE¼NE¼ sec. 25, T. 16 N., R. 6 E), is greater than 90 m

## TERTIARY ROCKS

Tertiary and older bedrock units on the map were mapped using the Kern PG-2 stereoplotter in the Denver Geologic Division photogrammetry laboratory. Contacts were compiled from aerial photographs: 1:16,000-scale color U.S. Forest Service photographs, 1:30,000-scale Bureau of Land Management and USGS black and white photographs, and 1:40,000-scale USGS NAPP (National Aerial Photography Program) black and white photographs. These contacts were field checked and revised by new geologic mapping. Contact relations and units were coordinated with geologic maps being prepared for the adjoining Montoso Peak (R.A. Thompson and R.R. Shroba, USGS, written commun., 1998), Cochiti Dam (D.P. Dethier, Williams College, written and oral commun., 1999), and Santo Domingo Pueblo (Smith and Kuhle, 1998) quadrangles. Substantial geologic map contact data, lithologic descriptions, and chemical analyses were compiled from the 1:15,840-scale geologic map of the La Cienega area by Brewster Baldwin (Sun and Baldwin, 1958). Previous studies of the Tetilla Peak area (Zimmerman and Kudo, 1979) and an early planimetric base geologic map of Los Cerrillos area by Disbrow and Stoll (1957) were also utilized to a lesser degree.

A modified version of the IUGS (International Union of Geological Sciences) total alkali-silica classification (Le Bas and others, 1986) was used in classifying the volcanic rocks of the Cerros del Rio volcanic field and older Oligocene-Miocene volcanic rocks. In this classification, the sum of Na<sub>2</sub>O and K<sub>2</sub>O are plotted against silica content, and arbitrary boundaries are drawn based on silica content to separate the common volcanic rock types basanite, basalt, basaltic andesite, andesite, and dacite (fig. 1). Rocks above 5 percent total alkalis for basalts, and above the inclined line ranging from 5 to 8 percent total alkalis for andesites and dacites have an alkalic root name (trachybasalt, basaltic trachyandesite, trachyandesite, and trachyte). Where volcanic rocks have greater than 2 percent Na<sub>2</sub>O minus K<sub>2</sub>O (table 3), they may be classified as sodic (sodic trachybasalt is hawaiiite); if less than 2 percent Na<sub>2</sub>O minus K<sub>2</sub>O, they may be classified as potassic (potassic trachybasalt). The potassic end-member of the trachyandesite compositional field is termed latite. Where units straddle boundaries between rock types, generally the range in IUGS rock names will be cited in the "Description of Map Units," but only one rock name is used for the name of the unit. Additional informal terms used in the "Description of Map Units" are:

- (1) transitional basalt—basalt that straddles the alkalic-subalkalic compositional boundary at 5 percent total alkalis, and has less than 2 percent normative nepheline;
- (2) alkaline basalt—trachybasalt with greater than 2 percent normative nepheline, and appearing gradational with a compositional series extending from basanite;
- (3) xenocrystic basaltic andesite—basaltic trachyandesite that is generally hypersthene-normative, and has resorbed quartz and plagioclase xenocrysts;
- (4) nephelinite—an undersaturated basanitic composition containing less than 41 percent silica; nephelinite is found only in the Oligocene-Miocene unit previously called the Cieneguilla Limburgite (limburgite is a synonym for a glassy basanite—LeMaitre and others, 1989), here redescribed as the Cieneguilla Basanite; and
- (5) latite—the potassic compositional end-member (Na<sub>2</sub>O–2<K<sub>2</sub>O) of the trachyandesite field; some monzonite porphyry also overlaps this range.

Most major-element chemical analyses (table 3) were done at the USGS Denver X-ray fluorescence (XRF) laboratory for major-elements by Dave Siems (all samples in table 3 whose sample numbers begin with 96D, 97D, 96T, and SM). A few analyses (with sample numbers assigned as beginning with 79ZK) were determined at the University of New Mexico by John Husler (Zimmerman and Kudo, 1979). Sun and Baldwin (1958) had several wet chemical analyses for igneous rocks of the La Cienega area done in the 1950's. These samples have sample numbers in table 3 that are assigned to begin with 58B, with the exception of 53SGTH27, which they reproduced from Stearns (1953b).

Some informal volcanic unit names are new, owing to the inadequacy of pre-existing names (Stearns, 1953a, b; Kelley, 1978) to relate lava flows and domes to specific vent locations. Units of the Cerros Del Rio volcanic field were subdivided based upon interpreted monogenetic volcanic centers wherever possible. Cinder in cinder cones is shown by a stipple pattern on top of the color assigned to that specific basalt stratigraphic unit. Dikes and cinder located together indicate a vent area for a particular basalt unit. The basalt of Mesita de Juana (Tbj) is a new informal name for the basaltic shield volcano south of Cañada de Santa Fe; the cinder cone vent for the volcano is just north of Interstate 25. The Mesita de Juana volcano is derived from the place name Mesita de Juana Lopez Grant. The Juana Lopez name has already been used for a member of the Mancos Shale by Dane and others (1966). The basalt of Tsinat Mesa (Tbs) is informally named from the extreme south end of a flow erupted from the basaltic vent at the northeast corner of the Tetilla Peak quadrangle. The basalt of La Bajada (Tbb) is the informal name for basalts that form the rim of the La Bajada escarpment, at least some of which

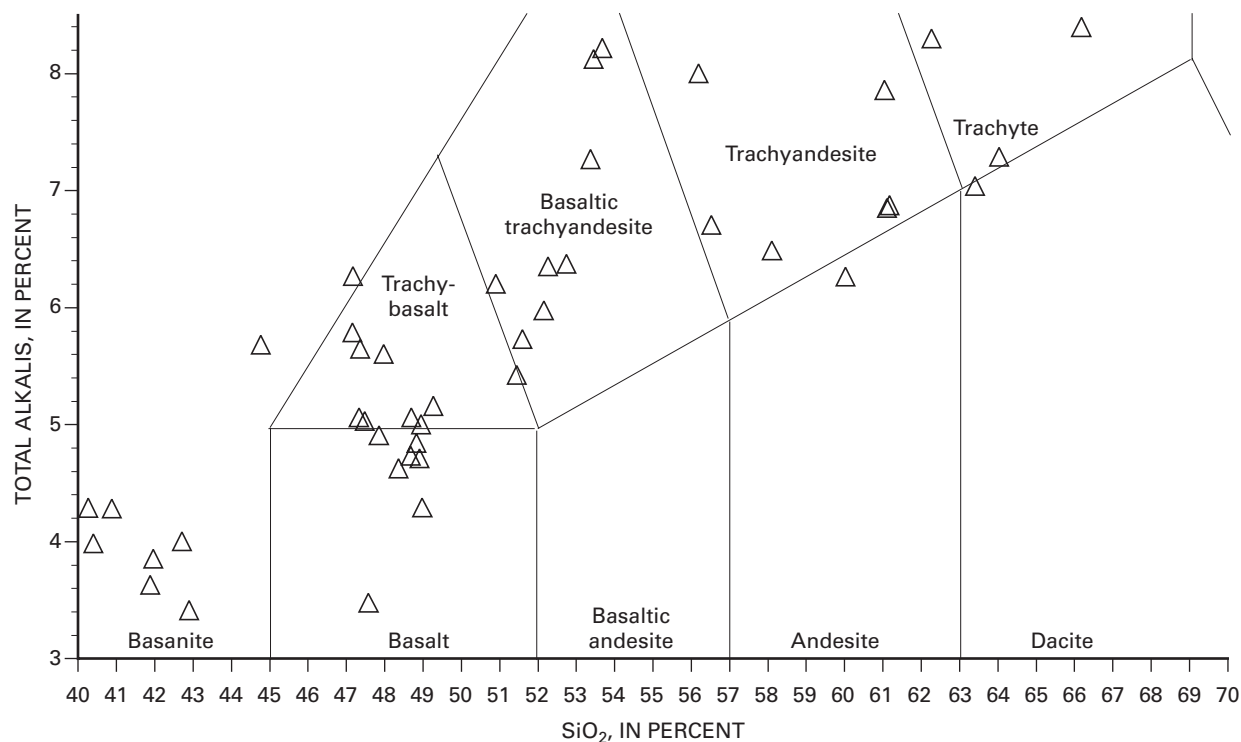


**Figure 1.** IUGS (International Union of Geological Sciences) total alkali-silica classification.

were erupted from the cinder cone immediately southwest of Tetilla Peak. Basalts of the Caja del Rio (Tbr) are erupted from many vents within the Cerros del Rio volcanic field. The southern part of the plateau formed by these eruptions occurs in the Tetilla Peak quadrangle north of the Santa Fe River, but most of the vents and flows are located to the north in the Montoso Peak quadrangle. Detailed correlation of flows to vents for the basalts of the Caja del Rio awaits synthesis of the Cerros del Rio volcanic field stratigraphy, incorporating geology on the Tetilla Peak, Montoso Peak, Cochiti Dam, Santo Domingo Pueblo, and White Rock quadrangles (R.A. Thompson, D.A. Sawyer, USGS, and D.P. Dethier, Williams College, unpub. data, 1999). The first letter of the symbol for the Cerros del Rio volcanic field stratigraphic units represents age (T for Tertiary for these Pliocene-Oligocene volcanic rocks), the second letter represents composition (b for basalt, a for andesite, d for dacite), and a third arbitrary letter relates the geographic name to the vent area (for example, Tbj for the basalt of Mesita de Juana).

All  $^{40}\text{Ar}/^{39}\text{Ar}$  age determinations were provided by Dr. William C. McIntosh, New Mexico Geochronology Research Laboratory, N. Mex. Institute of Mining and Technology, Socorro, N. Mex. Ages and uncertainties are listed at the bottom of table 3 and in table 4 for the samples that have been determined. Ages were measured on whole rocks from the basalts, and from hornblende in the andesite and dacite of Tetilla Peak. Most  $^{40}\text{Ar}/^{39}\text{Ar}$  uncertainties were less than 150 ka (0.15 Ma), except for both hornblendes (samples 96DTP10 and 96TTP01), and one basalt (table 3, sample 96DTP09). This basalt sample had a disturbed age spectrum and a larger uncertainty (350 ka, 0.35 Ma) greater than any other basalt whole-rock age. The Tetilla Peak hornblendes had similar large uncertainties (210–270 ka: 0.21–0.24 Ma) and their ages do not agree with mapped stratigraphic relations. However, considering the uncertainties they are not analytically distinct from the other Cerros del Rio  $^{40}\text{Ar}/^{39}\text{Ar}$  basalt ages from the Tetilla Peak quadrangle.

Interpretation of a new aeromagnetic survey flown at 400-m spacing and 150-m height above the Cochiti Pueblo and western/central parts of the Cerros del Rio volcanic field (U.S. Geological Survey and others, 1999) has generated preliminary indications of paleomagnetic remanent polarity for the igneous rocks of the Tetilla Peak quadrangle. These preliminary interpretations of magnetic polarity (V.J.S. Grauch, USGS, oral commun., 1998) are included in the map unit descriptions of the Cerros del Rio volcanic field. Preliminary paleomagnetic investigations of these rocks have largely confirmed the magnetic polarity of volcanic map units interpreted from the aeromagnetic data (Mark Hudson and Melanie Hopkins, USGS, written commun., 2000). Basalts of the Cerros del Rio volcanic field show apparent normal and reversed magnetic polarities. Magnetic lows indicative of reversed magnetic polarity are clearly caused by acquisition of intrinsic magnetization when the lava cooled and the Earth's magnetic pole was located near the South Pole in Antarctica. Magnetic highs are formed when lava flows or intrusions were erupted and cooled during a time in the geologic past when the Earth's magnetic field was located near the present-day north magnetic pole, or by a relatively high magnetite content of the rocks causing an induced magnetic field today, or due to both effects.

Apparent magnetic polarity of the rocks can be estimated when the magnetic signature of the total aeromagnetic field correlates with topography or a mapped geologic contact boundary. Some lava flow boundaries show a clear correspondence to magnetic lows, and these are interpreted to be reversely magnetized rocks. Other positive anomalies show excellent correspondence to topographic features, such as the positive magnetic high located at the summit and the shoulders of Tetilla Peak. Magnetic highs are also present where intrusive bodies or dikes intrude cinder cones as at the Mesita de Juana vent; in this case the high may be due to intrusive rocks in the subsurface inducing a normal (positive) field. There is also evidence for magnetic highs corresponding to older Tertiary monzonite intrusions, as in the western part of Cañada de Santa Fe, just east of the village of La Bajada. A very large positive magnetic anomaly is associated with the Cerrillos monzonite intrusive center, and with its outlier to the north at Cerro Seguro in the Tetilla Peak quadrangle. Aeromagnetic anomalies may also indicate buried igneous bodies, such as an interpreted basaltic vent beneath the flood plain of the Santa Fe River in the adjoining Santo Domingo Pueblo quadrangle to the west (V.J.S. Grauch, USGS, and G.A. Smith, University of New Mexico, oral commun., 1998). The single audio-magneto-telluric (also referred to as high-frequency magnetotelluric) sounding, AMT-4, was obtained by Brian Rodriguez (USGS, written commun., 1998).

#### Volcanic rocks of the Cerros de Rio volcanic field

- Tby** **Younger basalt of Caja del Rio (Pliocene)**—Transitional basalt and trachybasalt cinders erupted from a group of as many as six cinder cones east of Tetilla Peak. Sparsely to moderately olivine-phyric, these basalts are transitional between weak normative hypersthene (<2 percent hy) and nepheline (<2 percent ne) types. Aeromagnetic data suggest that the northernmost vent on the Tetilla Peak quadrangle and associated lava may be normal and thus possibly erupted during the Reunion Subchron (Berggren and others, 1995a). Preliminary paleomagnetic data (M.R. Hudson and M. Hopkins, USGS, written commun., 2000) at a locality just north of the Tetilla Peak quadrangle support this interpretation
- Tbd** **Basaltic dikes (Pliocene and Miocene)**—Local dikes, sills, and irregularly shaped basaltic intrusions that cut cinder deposits of Pliocene age in Cerros del Rio volcanic field. Some basaltic dikes cutting older Tertiary, Cretaceous, and Jurassic rocks in southern part of quadrangle are probably related to the Cieneguilla Basanite (Tc)
- Tbr** **Basalt of Caja del Rio (Pliocene)**—Basalt lava flows and dikes of the Caja del Rio are mainly alkaline basalts and trachybasalts, containing sparse olivine phenocrysts in a fine-grained glassy groundmass. A sample of a dike (96DTP12) yielded an  $^{40}\text{Ar}/^{39}\text{Ar}$  age of  $2.42 \pm 0.03$  Ma consistent with eruption during the early Matuyama Reversed-polarity Chron. Cinder cone deposits that the dike cuts have an apparent reversed magnetic polarity that supports a reversed Matuyama magnetostratigraphic assignment. Compositions of lavas are only sparingly characterized, but one analyzed sample (96DTP05) is a moderately silica-undersaturated basanite (8.1 percent normative ne). An  $^{40}\text{Ar}/^{39}\text{Ar}$  age of  $2.35 \pm 0.06$  Ma for this flow is also consistent with apparent reversed magnetic polarity and eruption age during the early Matuyama Chron. Preliminary paleomagnetic data (M.R. Hudson and M. Hopkins, USGS, written commun., 2000) confirm the reversed magnetic polarity of basalts in this unit. A poorly constrained  $^{40}\text{Ar}/^{39}\text{Ar}$  age of  $2.03 \pm 0.35$  Ma of one sample (96DTP09) from this unit is probably too young. Similar-aged basaltic rocks are widespread to the northwest in White Rock Canyon (Woldegabriel and others, 1996). Unit includes cinder deposits (shown by pattern) consisting predominantly of oxidized cinders, scoria, blocks, and bombs, cut by dikes and sills (only locally depicted) of fine-grained basalt, trachybasalt, and basaltic trachyandesite. Locally quarried for cinder block and decorative cinder. Thickness of Caja del Rio basalts is at least 60 m in the quadrangle, and perhaps more than 150 m thick at the north edge of the map area
- Tdt** **Dacite of Tetilla Peak (Pliocene)**—Thin, cone-forming, small-volume, light-grayish-tan, low-silica dacite (63.4–64 percent  $\text{SiO}_2$ ) lava capping Tetilla Peak. Dacite represents the most-differentiated magma composition in the eastern Cerros del Rio volcanic field. Phenocrysts of hornblende and plagioclase are conspicuous. Attempts to date hornblende by  $^{40}\text{Ar}/^{39}\text{Ar}$  were unsuccessful, yielding an age of  $2.78 \pm 0.27$  Ma, which is too old based on stratigraphic position relative to isotopic ages on subjacent basalt of La Bajada (Tbb) and overlying younger basalt of Caja del Rio (Tbr). Strong correlation of a positive magnetic anomaly with the summit topography of Tetilla Peak suggests a normal polarity for the andesite (Tat) and dacite (Tdt) of Tetilla Peak. Age is probably about 2.60–2.65 Ma, based upon relative magnetostratigraphic position for eruption prior to the Gauss-Matuyama boundary
- Tat** **Andesite of Tetilla Peak (Pliocene)**—Massive light-gray lava flows that form most of Tetilla Peak. The upper surface of flows west and north of Tetilla Peak have conspicuous concentric flow ridges that are concave toward Tetilla Peak, indicating northwesterly



flow. Andesite lavas (56.5–62.7 percent SiO<sub>2</sub>) range in composition from latite (relatively potassium rich) to trachyandesite based on IUGS classification. Mineralogy in hand specimen is dominated by common plagioclase and clinopyroxene phenocrysts, sparse xenocrystic quartz, and hornblende that locally is a prominent phenocryst in upper part of lava flows (Zimmerman and Kudo, 1979). Attempts to date hornblende by <sup>40</sup>Ar/<sup>39</sup>Ar were unsuccessful, yielding an age of 3.04±0.21 Ma, which is too old based on stratigraphic position relative to isotopic ages on subjacent basalt of La Bajada (Tbb). Age probably about 2.60–2.65 Ma based upon relative magnetostratigraphic position prior to Gauss-Matuyama boundary. The strong correlation of a positive magnetic anomaly with topography on the summit of Tetilla Peak suggests a normal polarity for the andesite (Tat) and dacite (Tdt) of Tetilla Peak. Preliminary paleomagnetic data (M.R. Hudson and M. Hopkins, USGS, written commun., 2000) confirm the normal magnetic polarity of this unit. Individual flows range from 50 to 70 m in thickness; aggregate thickness as much as 200 m

- Tbs **Basalt of Tsinat Mesa (Pliocene)**—Basalt lava flows and dikes erupted from cinder cone(s) and vents at the northeast corner of the Tetilla Peak quadrangle were the source for the basalt of Tsinat Mesa. It forms the eastern rim of the Cerros del Rio volcanic field adjoining the village of Cieneguilla in the Turquoise Hill and Tetilla Peak quadrangles. These basaltic lavas overlie the Ancha Formation (QTa) (Spiegel and Baldwin, 1963). The initial deposits of the Cerros del Rio volcanic field are hydromagmatic basaltic tephras, erupted from some vents to the west that were probably buried by younger lavas and sediments. A basal lava flow 4–6 m thick was deposited on the Ancha, and is overlain by as many as one to two additional flows of similar thickness that flowed south as far as the southeast side of Las Tetillitas (7–8 km). The lowest flow is a moderately undersaturated [normative nepheline (ne) 5.5 percent] trachybasalt in composition, and can be classified as a hawaiite based on IUGS criteria (Le Bas and others, 1986). The second and subsequent flows, as well as cinder deposits and dikes exposed in the cinder quarry in sec. 18, T. 16 N., R. 8 E., are fine-grained xenocrystic trachybasalt to basaltic trachyandesite (51–53 percent SiO<sub>2</sub>), with small olivine phenocrysts and common resorbed plagioclase and quartz xenocrysts. Unit includes cinder deposits (shown by pattern) consisting predominantly of oxidized cinders, scoria, blocks, and bombs, cut by dikes and sills (only locally depicted) of fine-grained basalt, trachybasalt, and basaltic trachyandesite. Cinder deposits are locally quarried for cinder block and decorative cinder. A dike cutting the xenocrystic basaltic trachyandesite gave an <sup>40</sup>Ar/<sup>39</sup>Ar isotopic age of 2.68±0.03 Ma. Preliminary paleomagnetic data (M.R. Hudson and M. Hopkins, USGS, written commun., 2000) confirm the normal magnetic polarity of this unit. Exposed thickness is only about 20–30 m, but it could thicken to the west where covered by younger basalts
- Tbb **Basalt of La Bajada (Pliocene)**—Basalt lava flows and dikes limited to exposures along western escarpment (La Bajada) rim north of the Santa Fe River; thin (4–15 m thick) flows are offset by the La Bajada fault zone. Typically consists of one to three lava flows of fine-grained trachybasalt (potassic trachybasalt by IUGS criteria of Le Bas and others, 1986), containing common to abundant olivine phenocrysts. Includes minor local exposures of stratigraphically older basalt, basaltic andesite, and andesite beneath basalt of La Bajada in canyons cutting the western escarpment. Lowest basalt west-southwest of Tetilla Peak yielded an isotopic age of 2.62±0.14 Ma. Includes a local, nearly aphyric, glassy andesite flow in major canyon south of Tetilla Peak in unsurveyed section 32. Unit may thicken to the north and east based upon limited exposures in western canyons and in Tetilla Arroyo to the north, and by significant thickening of Cerros del Rio basalts (to 200–250 m thick) in the 1,200-ft (366 m) well in the Montoso Peak quad to the north
- Tbj **Basalt of Mesita de Juana (Pliocene)**—Basalts erupted on the southern side of the Cerros del Rio volcanic field, from vents located south of the Santa Fe River on the Mesita de Juana Lopez Grant. The Mesita de Juana volcano consists of three or four stacked flows forming a discrete basaltic shield, south of the Santa Fe River. A prominent, solitary cinder cone just north of Interstate 25 was the vent for latest flows erupted from the Mesita de Juana volcano. Unit includes cinder deposits (shown by pattern) consisting predominantly of oxidized cinders, scoria, blocks, and bombs, cut by dikes and sills (only locally depicted) of fine-grained basalt, trachybasalt, and basaltic trachyandesite. Locally quarried for cinder block and decorative cinder. Mesita de Juana basaltic rocks range in composition from basanite in the lowest flow to trachybasalt in the uppermost flows and dikes. The basanite flow is strongly undersaturated (normative ne 10.8 percent); trachybasalts are moderately undersaturated (ne 3.6–3.9 percent) and relatively enriched in sodium. The basanite has sparse olivine phenocrysts and minor quartz xenocrysts, whereas the trachybasalts have common olivine phenocrysts. Basal flow on the La

Bajada escarpment (sample 96DTP13) dated by  $^{40}\text{Ar}/^{39}\text{Ar}$  yields an isotopic age of  $2.66\pm 0.08$  Ma; a dike cutting late cinder cone (sample 96DTP15) gave an age of  $2.69\pm 0.08$  Ma. These new results are consistent with an earlier age determination of  $2.8\pm 0.1$  Ma (Bachman and Mehnert, 1978) on a Mesita de Juana flow at the southern rim of the Cerros del Rio volcanic field. Mesita de Juana basalts are normally magnetized based upon their aeromagnetic signature; preliminary paleomagnetic data (M.R. Hudson and M. Hopkins, USGS, written commun., 2000) confirm a normal magnetic polarity for this unit. This magnetic character is consistent with the new  $^{40}\text{Ar}/^{39}\text{Ar}$  ages indicating eruption during the Gauss-normal polarity Chron. Thickness of Mesita de Juana flows varies from a single 2- to 3-m-thick flow on the distal margins of the volcano to a composite thickness of as much as 40–55 m near the center of the shield (Peery and Pearson, 1994). Thickness of basalt is probably less than 15–20 m over most of shield

Miocene to Eocene igneous and sedimentary rocks

- Tsp** **Santa Fe Group—eastern piedmont facies (Miocene?)**—Piedmont fan deposits derived from the Sangre de Cristo Mountains, including axial-river deposits of the paleo-Santa Fe River. Predominantly massive, pink to buff, silty fine sand, cross-bedded fluvial sand, and subordinate amounts of pebble-cobble conglomerate, sandy silt, and mud. Clasts are principally moderately well rounded Precambrian pink and red granite, with subordinate subangular Tertiary monzonite, latite-andesite, and basalt derived from the Los Cerrillos intrusions, the Espinazo Formation, and possibly from the Cieneguilla Basanite. Unit Tsp commonly has dips of  $5^{\circ}$ – $10^{\circ}$  and is tilted due to movement of west-dipping normal faults. It is principally found beneath the rim basalts along the La Bajada escarpment. Lithology and composition of this unit are similar to those of the untilted Ancha Formation (QTa), the eastern piedmont facies of the Sierra Ladrones Formation (Smith and Kuhle, 1998), and may be correlative in part with some of the Tesuque Formation (Spiegel and Baldwin, 1963). Maximum exposed thickness about 70 m in major arroyo southwest of Tetilla Peak, but typically much less (20–30 m)
- Tab** **Abiquiu Formation (Miocene to Oligocene)**—Light-gray, ash-rich silty sand and silt beds that form prominent cliffs (85 m high) immediately north of Santa Fe River, near the village of La Bajada. The section consists of reworked ash and contains a few primary ash-fall beds (0.2–0.5 m thick), but is largely reworked ash admixed with detrital silty mud and minor arkosic sand. Lower part of unit Tab, exposed between Interstate 25 and La Bajada, locally contains thin limestone beds interbedded with gray, green, and red silt and clay, which were interpreted by Stearns (1953a) to be lacustrine in origin. The volcanoclastic deposits at La Bajada are tentatively correlated as a distal equivalent of the volcanoclastic Abiquiu Formation (Stearns, 1953a) exposed in the Abiquiu area about 70 km north of the map area. Stearns (1953a) also suggested a possible correlation with the Zia Sand in the Jemez River area about 45 km west of the map area. Total thickness about 300 m
- Tc** **Cieneguilla Basanite (Miocene to Oligocene)**—Medium- to dark-gray basanite, nephelinite, and minor basalt (Cieneguilla Limburgite of Stearns, 1953b) flows, and interbedded volcanoclastic and epiclastic sediments. It also forms north- to north-northeast-striking dikes (and a few small and irregular sills) cutting older rocks on the west side of the La Bajada escarpment, in the Cañada de Santa Fe, and south of the Mesita de Juana vent extending on to the Madrid quadrangle. It is stratigraphically above the Espinazo Formation (Te) on the northeast side of the Tetilla Peak quadrangle in the Cañada de Santa Fe near Cañon. The type section for the Cieneguilla Basanite was defined in the Cañada de Santa Fe between Cieneguilla and Cañon, and Stearns (1953b) measured it there as 180 m thick. A more detailed section measured by Brewster Baldwin (Sun and Baldwin, 1958, p 17, fig. 3) indicated a thickness of 220 m. Four cliff-forming packages of two to five discontinuous flows (each flow about 3–9 m thick) are interspersed with subordinate basaltic tephra and volcanoclastic sediments.

Non-vesicular basanite and basalt typically have moderate to abundant olivine (10–15 percent), lesser clinopyroxene (5 percent) phenocrysts; sparse, small plagioclase phenocrysts occur in the basalt. Granular groundmass mineralogy consists of olivine, clinopyroxene, nephelinite, biotite, and zeolites (natrolite and gonnardite: Baldrige, 1979). Basanite lava flows locally contains small (as large as 10 cm) ultramafic inclusions of harzburgite and minor granulite, and megacrysts of titaniferous magnetite, and both green and black clinopyroxenes. The green clinopyroxene megacrysts include nephelinite and are similar in composition to phenocrysts in the host basanite (Baldrige, 1979). Age of the Cieneguilla basanite was determined by Baldrige and others (1980) as  $25.1\pm 0.7$  Ma by whole rock K-Ar. However, they also obtained Miocene K-Ar ages of  $19.5\pm 0.5$

Ma on biotite and  $19.6 \pm 0.6$  on “feldspar” from the underlying latite of the Espinaso Formation, which, if correct, would allow a possible Miocene age for the Cieneguilla Basanite. Either the age they determined for the Espinaso or the Cieneguilla must be in error, for they conflict with the stratigraphic constraints. The basanite section dips about  $15^\circ$  NE, and was deposited before the 2.5–3 Ma age of the flat-lying basalts capping La Bajada to the west. It is tilted roughly the same amount as the underlying latites in the upper part of the Espinaso Formation

Te

**Espinaso Formation (Miocene or Oligocene)**—Predominantly consists of partly to completely brecciated lava flow lithologies in the area of La Cienega. More distal volcanoclastic sedimentary rocks and breccias are exposed to the west along the La Bajada escarpment, and are similar to lithologies that characterize the Espinaso farther south in the Los Cerrillos and Espinaso Ridge areas (Erskine and Smith, 1993). Brewster Baldwin subdivided the Espinaso in the La Cienega area into three map units—a lower andesite unit and two compositionally distinct latite units exposed only northeast of La Cienega (Sun and Baldwin, 1958). The andesite unit is gray to red brown and includes some fragmental lava clasts consisting of porphyritic hornblende-plagioclase andesite. The andesite typically has conspicuous hornblende phenocrysts, and the dominant lithology consists of fragmental breccias (locally welded) and proximal volcanoclastic deposits. It was deposited prior to the intrusion of the Cerro Seguro augite monzonite (Tmi). There may be an angular unconformity between upper Espinaso latites and the lower andesite breccia unit of the Espinaso Formation, as well as a possible unconformity between the upper Espinaso latites and the Cieneguilla Basanite (Sun and Baldwin, 1958). Both latite compositions (the “calcic” latite and “glassy” latite of Sun and Baldwin, 1958) are brownish-gray fragmental latite breccias with little intact lava-flow lithology preserved. In the southwestern part of the quadrangle along the La Bajada escarpment, the Espinaso mainly consists of clast-supported volcanic and sedimentary breccia containing andesite or latite clasts. The unit in this area also includes subordinate interbedded volcanoclastic sedimentary rocks. The age of the Espinaso is not well constrained by published isotopic ages. Baldrige and others reported Miocene K-Ar ages of  $19.5 \pm 0.5$  Ma on biotite and  $19.6 \pm 0.6$  on “feldspar” from the uppermost latite of the Espinaso Formation. These results are inconsistent with the 25.1 Ma Oligocene age determined for the overlying Cieneguilla Basanite. By correlation with the similar mineralogy and chemistry of the younger Cerrillos augite monzonite intrusion, an age of 28–30 Ma might be expected for the upper Espinaso latite flows. The age of the intrusions thought to correspond to the hornblende andesite lavas is 36–31 Ma, as described above. The andesite unit was estimated at 180 m in thickness by Sun and Baldwin (1958) and the two latites are each greater than 120 m in thickness

Tmi

**Monzonite and monzonite porphyry intrusions (Oligocene)**—Pinkish-brown to medium-gray, fine-grained intrusions and dikes of sub-volcanic monzonite porphyry and monzonite exposed at Cerro Bonanza, Cerro Seguro, Cerro Tetillitas, and in the Cañada de Santa Fe. The monzonite porphyry intrusion centered on Cerro Seguro appears to have domed both the Galisteo Formation (Tg) and lower Espinaso Formation (Te) andesite at the margins of the pluton; contacts against older rocks are faults. Cerro Seguro and Cerro Bonanza intrusions are augite-biotite monzonite (Stearns, 1953a; Sun and Baldwin, 1958). Phenocrysts are plagioclase and augite in a fine-grained groundmass of orthoclase, plagioclase, biotite, and magnetite. Phenocrysts of augite 1–2 mm in size form as much as 8 percent of the rock, but are often destroyed by alteration and weathering. Disbrow and Stoll (1957) correlated both intrusions with the latest stage of Cerrillos intrusive activity, their Ti4 phase augite-biotite monzonite intrusions. The augite-biotite monzonite in Cerro Bonanza and Los Cerrillos, and the augite-biotite monzonite porphyry of Cerro Seguro, differ primarily in texture. The central Cerrillos monzonite is nearly holocrystalline, whereas the Cerro Seguro monzonite porphyry stock is strongly porphyritic; orthoclase in both varieties is restricted to the groundmass or finer grained matrix. A single analyzed sample (58BTP84 from Sun and Baldwin, 1958) of Cerro Seguro augite monzonite porphyry (table 3) plots in the trachyandesite (or latite, a potassium-rich trachyandesite) field of the total-alkali/silica plot (fig. 1). The chemistry of the augite monzonite porphyry intrusion is similar to that of the latite lavas mapped by Sun and Baldwin (1958), and clearly distinct from the andesite lava that is stratigraphically the lowest unit of the Espinaso Formation. The composition of the latites is closer to the alkaline end-member compositions described by Erskine and Smith (1993) for younger volcanic sediment clasts in the Espinaso Formation. The augite monzonite porphyry intrusion at Cerro Seguro had been dated by Baldrige and others (1980) at  $30.2 \pm 0.7$  Ma by K-Ar on biotite. It has recently been dated by an  $^{40}\text{Ar}/^{39}\text{Ar}$  plateau age spectrum on biotite at  $29.40 \pm 0.05$  Ma (Sauer, 1999). The Cerro Seguro stock correlates with

- augite monzonite intrusions at Cerro Bonanza and other localities in Los Cerrillos that have been dated as approximately 28–30 Ma in age (Maynard, 1995; Sauer, 1999)
- Tmh Hornblende monzonite porphyry (Oligocene)**—Small exposures of gray hornblende-bearing monzonite porphyry intrusions flanking the northwest side of Cerro Bonanza. Phenocrysts consist of equant plagioclase and prismatic black hornblende crystals set in a dark-gray holocrystalline groundmass. Probably correlative with phase Ti1 of Disbrow and Stoll (1957), having mineralogy (hornblende and plagioclase phenocrysts set in a groundmass that also contains orthoclase, quartz, augite, sphene, and magnetite) and chemistry typical of the early metaluminous Cerrillos intrusions and the lower Espinaso Formation lavas (Erksine and Smith, 1993). If this correlation is correct, its age may be close to the 36–34 Ma age of the metaluminous intrusions in the Ortiz Mountains located to south of the Los Cerrillos intrusive center, across the Galisteo River (Maynard, 1995; Erskine and Smith, 1993). Hornblendes from this intrusive suite in the Ortiz Mountains, San Pedro Mountains, and South Mountain to the south have recently been dated from 36 to 31 Ma in age by  $^{40}\text{Ar}/^{39}\text{Ar}$  age spectrum and isochron methods (Sauer, 1999)
- Tg Galisteo Formation (Oligocene and Eocene)**—Red to brownish-yellow sandstone, red mudstone, and conglomerate exposed in the south half of the quadrangle. Sandstones range from yellow to red, well-sorted, fine sandstone to coarse-grained red, more poorly sorted, silty fine-grained sandstone. Conglomerate clasts include white, gray, and black chert pebbles, gray limestone cobbles and pebbles, red granite, schist, and rare petrified wood. The Galisteo crops out in three distinct areas of the quadrangle: (1) southwest-dipping beds in the vicinity of La Cienega; (2) in the Cañada de Santa Fe midway between La Cienega and La Bajada, northeast-dipping beds disconformably overlie the Mancos Shale; and (3) near Interstate 25 at the base of the La Bajada escarpment, the Galisteo is exposed in a complex series of fault blocks underlying the Pliocene basalt flows. The Galisteo in the Tetilla Peak quadrangle correlates with the upper part of the Galisteo Formation and does not include any of the recently defined Paleocene Diamond Tail Formation (Lucas and others, 1997; S.M. Cather, oral commun., 1998). The Galisteo is interpreted to be a synorogenic sedimentary deposit coeval with the Laramide orogeny in this part of New Mexico (Cather, 1992), and thickness varies greatly in the region due to Eocene as well as subsequent Oligocene deformation. The Galisteo has a maximum thickness of as much as 980 m near Cerrillos and Galisteo just to the south in the Madrid quadrangle. Brewster Baldwin measured a thickness of 400 m for the Galisteo along Cienega Creek in the eastern part of the quadrangle (Sun and Baldwin, 1958). The Galisteo in the Cañada de Santa Fe is relatively unfaulted with its basal contact disconformably overlying the Mancos Shale, and is conformably overlain by Espinaso Formation in the Cañada de Santa Fe. The Galisteo here has consistent 12° ENE dip indicates a thickness of about 220 m

## MESOZOIC SEDIMENTARY ROCKS

- Mancos Shale (Upper Cretaceous)**—Consists of thick deposits of shale, calcareous shale, sandy shale, and minor limestone and bentonite beds deposited in marine conditions. The Mancos regionally intertongues with continental deposits of the Upper Cretaceous Crevasse Canyon Formation, and is overlain by the Upper Cretaceous Mesaverde Group, but these units are not exposed in the Tetilla Peak quadrangle. The uppermost Mancos exposures are equivalent to what Bachman (1975) termed the Niobrara Member of the Mancos in the Madrid quadrangle to the south. Although regionally the Niobrara-equivalent part of the Mancos contains local silty sand beds, mappable contacts of a sand-rich lentil mapped by Bachman could not be identified on the Tetilla Peak quadrangle. Members of the Mancos here are subdivided in part based on a proposed principal reference section for the Mancos Shale (Leckie and others, 1997) located north of Mesa Verde National Park in Colorado. These members of the Mancos correlate with formal stratigraphic units for the Cretaceous Western Interior Seaway deposits of Colorado and western Kansas (that is, Bridge Creek Limestone Member rather than Greenhorn Limestone Member of the Mancos Shale). The Mancos in the area of the Galisteo Creek watershed is approximately 600–700 m thick (Bachman, 1975; D.A. Sawyer and W.A. Cobban, unpub. data, 1998)
- Kmn Niobrara Member**—Consists of shale, calcareous shale, mudstones, and thin sands that lie above calcarenitic limestone of the Juana Lopez Member. The upper part of the exposed Mancos section consists of yellowish-brown to olive-gray silty or sandy shale with interbedded sandstone beds containing yellowish-brown ovoid calcareous concretions as large as 0.6–0.9 m in diameter; it grades downward into lower Niobrara equivalents. These sandstone beds in the upper Niobrara Member (equivalent to the

Cortez Member of Leckie and others, 1997) may represent distal facies related to the El Vado Sandstone Member of the Mancos in the Tierra Amarilla/Chama Basin area (Landis and Dane, 1967). They may also be correlative with the Dalton Sandstone Member of the Crevasse Canyon Formation and the Hosta Tongue of the Point Lookout Formation in the Hagan Basin (Black, 1979) and the eastern San Juan Basin (Molenaar and Baird, 1992). The lower part of the Niobrara-equivalent Mancos corresponds to the Montezuma Valley and Smoky Hill Members of Leckie and others (1997). It is a medium- to light-olive-gray chalky/limy calcareous shale and mudstone with scattered marlstone beds. The erosional unconformity corresponding to the Smoky Hill/Montezuma Valley Member boundary has not been identified east of the Rio Grande rift to date (that is, the contact corresponding to the “Basal Niobrara” unconformity in the San Juan Basin of Molenaar and Baird, 1992). The uppermost Mancos Shale is eroded and overlain with minor unconformity by the Eocene Galisteo Formation (Tg) in the Cañada de Santa Fe. The thickness of the Niobrara Member is greater than the exposed 370 m, but less than the 520-m section in the Madrid quadrangle to the south where Mesaverde Group sedimentary rocks conformably overlie the Mancos. A thickness of 430 m in the quadrangle is probably a reasonable estimate. Faults concealed beneath the Cerros del Rio volcanic field may increase the apparent thickness of the Mancos based on surface outcrops (Peery and Pearson, 1994). A north-plunging synclinal hinge formed in response to Tertiary intrusion around the Cerrillos monzonite intrusive center (Stearns, 1953b) interrupts the east-dipping homocline of Mesozoic units and limits the amount of Niobrara exposed to approximately the stratigraphic level of the Dalton Member/Hosta Tongue. The overlying Satan Tongue is not exposed in the Tetilla Peak quadrangle or north of Galisteo Creek in the Madrid quadrangle

- Kmj **Juana Lopez Member, and Blue Hill and Fairport Members of the Carlile Shale, undivided**—Highly fossiliferous limestone marker bed and underlying calcareous shale and clay shale. The Juana Lopez marker bed is about 3 m thick and consists of an orangish-brown-weathering calcarenite made up of calcareous fossil material. Identified species include the ammonite *Scaphites whitfield*, the oyster *Nicaiosolopha lugubris*, and *Inoceramus perplexus* (W.A. Cobban, USGS, oral commun., 1998). The map unit includes subjacent members of the Carlile Shale (Blue Hill and Fairport Members). The lower parts of the unit include noncalcareous olive-gray to dark-gray shale and silty shale equivalent to the Blue Hill Member of the Carlile Shale, underlain by medium-gray calcareous shale equivalent to the Fairport Member of the Carlile Shale. The type locality of the Juana Lopez Member of the Mancos is located 2 km south of the Tetilla Peak quadrangle in the Madrid quadrangle (Dane and others, 1966). The map unit, including the Blue Hill and Fairport Members, is about 110 m thick based on exposures at the south border of the Tetilla Peak quadrangle and adjoining parts of the Madrid quadrangle
- Kmb **Bridge Creek Limestone and Graneros Members, undivided**—Interbedded thin, medium-gray limestone (Bridge Creek Limestone) and light- to dark-olive gray calcareous shale (Graneros Member). Bridge Creek limestone beds are about 11 m thick. The total unit thickness is about 50 m including poorly exposed dark-gray sandy mudstone and silty shale of the Graneros Member that directly overlies the Dakota Sandstone (Leckie and others, 1997; Bachman, 1975)
- Kmd **Mancos Shale and Dakota Sandstone, undivided (Upper Cretaceous)**—Altered and contact-metamorphosed Cretaceous sandstone and shale adjacent to the Cerrillos monzonite intrusion at Cerro Bonanza on the southeast edge of the Tetilla Peak quadrangle. Correlation based on detailed geologic mapping in the Cerrillos by Disbrow and Stoll (1957)
- Dakota Sandstone (Upper Cretaceous)**—Stratigraphic usage for the Dakota Sandstone in north-central New Mexico is complex and at present only partially resolved, particularly east of the Rio Grande Rift. Our general usage follows Landis and others (1973), who summarized stratigraphic terminology for the intertonguing Dakota Sandstone and Mancos Shale in west-central New Mexico. The subdivisions of intertonguing Dakota Sandstone and Mancos Shale they describe from the Laguna area are, from top to bottom: the Two Wells Tongue of the Dakota Sandstone, the Whitewater Arroyo Tongue of the Mancos Shale, the Paguate Tongue of the Dakota Sandstone, the Clay Mesa Tongue of the Mancos Shale, the Cubero Tongue of the Dakota Sandstone, and the basal Oak Canyon Member of the Dakota Sandstone
- Kdc **Cubero Tongue**—Two stacked yellowish-brown, fine-grained calcareous sandstones, separated by minor discontinuous siltstone interbeds. The sandstone beds form a hogback that persists to the south through Galisteo Dam in the Madrid quadrangle (Bachman, 1975). The Dakota Sandstone here is correlated with the Cubero Member of

the Laguna type section (Landis and others, 1973) based on similar lithology and generally non-fossiliferous character. The ammonite *Acanthoceras alvaradoense* (S.G. Lucas, New Mexico Museum of Natural History, oral commun., 1999) has been found at the Galisteo Dam section in dark-gray shale and interbedded thin sandstone directly overlying the Cubero Tongue. This species is diagnostic for the Clay Mesa Tongue of the Mancos Shale, indicating that the underlying Dakota Sandstone unit must be the Cubero Tongue. Unit measures about 24 m in thickness

Kdo

**Oak Canyon Member**—Dark-gray, organic-rich clay shale and silty clay shale with beds of calcareous concretions, bentonite, and a basal conglomeratic sandstone. Calcareous concretions are reddish-brown ovoid masses as long as 0.5 m, and contain *Pycnodonte* sp. (W.A. Cobban, USGS, oral commun., 1998). These characteristics indicate correlation with the Thatcher Member of the Graneros Shale, and equivalence with the upper part of the Oak Canyon Member in the Laguna area (Landis and others, 1973). Presence of the Thatcher Member supports correlation of this section with the Oak Canyon Member rather than the Clay Mesa Tongue of the Mancos Shale. A thin (<2 m) bed of conglomeratic sandstone at the base of the shale disconformably overlies a prominent scour surface cut into the underlying Jackpile Sandstone Member of the Morrison Formation. This sandstone probably correlates with the Encinal Canyon Member of the Dakota (Aubrey, 1992), but it is not separated on this map. Map unit is approximately 18 m thick

**Morrison Formation (Upper Jurassic)**—Subdivisions of the Morrison Formation are commonly mapped in and adjoining the San Juan Basin, and have been recently described from the Hagan Basin (Lucas and others, 1995) and the San Ysidro–southeastern San Juan Basin areas (Anderson and Lucas, 1996, 1997). The members of the Morrison Formation that Lucas and Anderson described and correlated from these localities most proximal to the Tetilla Peak quadrangle are, from top to bottom: the Jackpile Sandstone Member, Brushy Basin Member, and Salt Wash Member. There is general consensus among all workers in New Mexico on nomenclature and characteristics of the Jackpile Sandstone and Brushy Basin Members. However, through decades of investigations in the Gallup-Grants-Laguna uranium belt of the southern San Juan Basin, the USGS and most workers in New Mexico have generally used the Westwater Canyon and Recapture Members (Condon and Peterson, 1986) for the lower part of the Morrison. This differs from the proposed usage of Lucas and Anderson (Lucas and others, 1995; Anderson and Lucas, 1996, 1997) that correlates approximately the same strata as the Salt Wash Member in the southeastern San Juan and Hagan Basins. The braided-stream fluvial environments represented by the Morrison are regionally contrasted with the underlying eolian and marginal marine saline deposits of the San Rafael Group. Lateral variability in rock types and the lack of a well-recognized unconformity between the sub-units of the Morrison has led to uncertainty and controversy over the stratigraphic assignments within the Morrison Formation (Condon and Peterson, 1986; Lucas and Anderson, 1995; Anderson and Lucas, 1996, 1997). In the Tetilla Peak quadrangle, all beds assigned to the Morrison are fluvial or lacustrine; no eolian beds are recognized. Total thickness of the Morrison Formation in the Galisteo monocline is about 250 m, consistent with surface exposures and drill-hole penetrations in the Hagan Basin of 238–276 m (Bruce Black, oral commun., 1999). The Morrison Formation is exposed only in the southwestern part of the quadrangle

Jmj

**Jackpile Sandstone Member**—White to pale-orange, kaolinitic, predominantly fine- to medium-grained, massive to cross-bedded fluvial sandstone (Owen and others, 1984). Generally moderately to poorly sorted subarkose with matrix clay; iron-rich staining and concretions common. Sandstone predominates, but discontinuous, thin, pale-olive to red-brown, clay-rich mudstone interbeds are locally present. Thickness about 70 m

Jmb

**Brushy Basin Member**—Variegated mudstone, silty mudstone, and minor sandstone that form strike valleys and slopes. Characteristic greenish-gray, pale-olive, grayish-brown, and pale-brown variegated thick and laterally continuous clay-rich beds with minor interbedded sand lenses. Subarkosic sand beds are yellowish gray and 25–80 cm thick. Proportion of sand to mud beds increases upward; thicker, more continuous sand beds in the upper part of the Brushy Basin Member form small hogbacks. Thickness about 120 m

Jmw

**Westwater Canyon Member**—Thickly bedded to massive grayish-yellow fluvial sandstone and lesser interbedded pale-brown to pale-olive mudstone. Sandstones are trough cross-bedded to massive subarkoses, and vary from fine- to medium-grained moderately sorted sands to coarse-grained poorly sorted sands in the upper part. Unit has a gradational contact with mudstones of the overlying Brushy Basin Member. Westwater Canyon as

- used here is generally equivalent to the Salt Wash Member as defined by Lucas and others (1995) and Anderson and Lucas (1997). Approximately 65 m thick
- Jwb**      **Wanakah Formation, Beclabito Member (Middle Jurassic)**—Heterogeneous set of beds that has a central conspicuously red to red-brown and grayish-red sequence of gypsiferous siltstones and sandstones that conformably overlies the gypsum member of the Todilto Formation. Stearns (1953a) described this sequence of Wanakah beds as “100–150 feet of maroon shale,” and as distinct from lithologies in the underlying gypsum of the Todilto Formation and the overlying Morrison Formation. Lucas and others (1995, 1997) have assigned this sequence of beds to the Beclabito Member of the Summerville Formation for the adjoining Hagan Basin and west to the Four Corners. The Bluff Sandstone Member of the Morrison has not been identified east of the Rio Grande rift to use as a marker between the Entrada Sandstone and Morrison Formation. The Summerville has in the past been used by the USGS for geologic mapping in the San Ysidro–Laguna area (Santos, 1975). However, more recent USGS usage has been to extend the Wanakah Formation into the western (Condon and Huffman, 1988) and southern San Juan Basin (Condon, 1989) for these Beclabito beds, and to restrict the Summerville Formation to Utah (O’Sullivan and Pierce, 1983). There is general agreement about the lithologic characteristics of the Beclabito Member interval and the underlying Todilto gypsum and limestone, which Condon and Huffman (1988) assigned to the Wanakah Formation. Disagreement persists between Lucas and other workers about the stratigraphic usage of the Beclabito Member, Wanakah and Summerville Formations, and the San Rafael Group. These distinctive red-brown sediments are approximately 30 m thick in the Tetilla Peak quadrangle
- Jt**      **Todilto Formation (Middle Jurassic)**—Conspicuous light-colored, ledge-forming unit consisting of a lower thin limestone member and an upper thick gypsum member (Kirkland and others, 1995; Lucas and Anderson, 1995) in the southwestern part of the quadrangle. The lower limestone is medium gray to yellow, thinly laminated to massive, and about 5 m thick. The gypsum member is white and massive, and pervasively brecciated where exposed at the surface. The original thickness is difficult to estimate due to surface weathering and dissolution; exposed thickness is about 30 m. Unit crops out as leached residuum intermixed with clay in weathered exposures of the Todilto; scattered coarse crystals (as long as 5–10 cm in length) of gypsum coat surface exposures. Gypsum was mined at the Rosario quarry from the same outcrop belt of Todilto Formation about 3 km south in the Madrid quadrangle
- Je**      **Entrada Sandstone (Middle Jurassic)**—Medium- to fine-grained, reddish-brown to yellowish-gray quartzose sandstone. The Entrada is a resistant ledge former and is massive to planar bedded, and displays cross-bedding at outcrop scale. The Entrada is divisible into subequal parts: a reddish-brown lower section and a predominantly yellowish-gray upper section, similar to that of the Hagan Basin farther to the south (Lucas and others, 1995). Exposed only in the southwest corner of the quadrangle; a more complete section exposed along Tom Payne Gulch immediately south in the Madrid quadrangle is 37 m thick
- Ƨc**      **Chinle Formation (Upper Triassic)**—Red-brown mudstone and siltstone; exposed section is incomplete, present only in fault blocks along the La Bajada fault zone in the southwest corner of the quadrangle. Bachman (1975) estimated at least 150 m of Chinle in more continuous exposures in the Madrid quadrangle to the south. The section in the Tetilla Peak quadrangle probably correlates with the Petrified Forest Member of the Chinle Formation

#### REFERENCES CITED

- American Geological Institute, 1982, Grain-size scales used by American geologists, modified Wentworth scale, in *Data sheets* (2nd ed.): Falls Church, Va., American Geological Institute, sheet 17.1.
- Anderson, O.J., and Lucas, S.G., 1996, Stratigraphy and depositional environments of middle and upper Jurassic rocks, southeastern San Juan Basin, New Mexico: *New Mexico Geological Society Guidebook, 47th Field Conference “Jemez Mountains Region”*, p. 205–210.
- 1997, The Upper Jurassic Morrison Formation in the Four Corners Region: *New Mexico Geological Society, 48th Field Conference “Four Corners” Guidebook*, p. 139–155.
- Aubrey, W.M., 1992, New interpretations of the stratigraphy and sedimentology of uppermost Jurassic to lowermost upper Cretaceous strata in the San Juan Basin of northwestern New Mexico: *U.S. Geological Survey Bulletin* 1808-J, 19 p.
- Bachman, G.O., 1975, Geologic map of the Madrid quadrangle, Santa Fe County, New Mexico: *U.S. Geological Survey Geologic Quadrangle Map GQ-1268*, scale 1:62,500.
- Bachman, G.O., and Mehnert, H.H., 1978, New K-Ar dates and the late Pliocene to Holocene geomorphic history of the central Rio Grande

- region, New Mexico: Geological Society of America Bulletin, v. 89, no. 2, p. 283–292.
- Baldrige, W.S., 1979, Mafic and ultramafic inclusion suites from the Rio Grande rift (New Mexico) and their bearing on the composition and thermal state of the lithosphere: Journal of Volcanology and Geothermal Research, v. 6, p. 319–351.
- Baldrige, W.S., Damon, P.E., Shafiqullah, M., and Bridwell, R.J., 1980, Evolution of the central Rio Grande rift, New Mexico—New Potassium-argon ages: Earth and Planetary Science Letters, v. 51, p. 309–321.
- Berggren, W.A., Hilgen, F.J., Langereis, C.G., Kent, D.V., Obradovich, J.D., Raffi, I., Raymo, M., and Shackleton, N.J., 1995a, Late Neogene (Plio-Pleistocene) chronology—New perspectives in high resolution stratigraphy: Geological Society of America Bulletin, v. 107, p. 1272–1287.
- Berggren, W.A., Kent, D.V., Aubry, M.P., and Hardenbol, J., eds., 1995b, Geochronology, time scales, and global stratigraphic correlations—A unified temporal framework for an historical geology: SEPM Special Publication 54, 386 p.
- Birkeland, P.W., 1999, Soils and geomorphology: New York, Oxford University Press, 430 p.
- Black, Bruce, 1979, Structure and stratigraphy of the Hagan embayment—A new look: New Mexico Geological Society Guidebook, 30th Field Conference “Santa Fe Country”, p. 101–105.
- Bryan, Kirk, and McCann, F.T., 1938, The Ceja del Rio Puerco—A border feature of the Basin and Range province in New Mexico, part II, Geomorphology: Journal of Geology, v. 46, p. 1–16.
- Cather, S.M., 1992, Suggested revisions to the Tertiary tectonic history of north-central New Mexico: New Mexico Geological Society, 43rd Guidebook, San Juan Basin IV, p. 109–122.
- Condon, S.M., 1989, Revisions of middle Jurassic nomenclature in the southeastern San Juan Basin, New Mexico: U.S. Geological Survey Bulletin 1808–E, 23 p.
- Condon, S.M., and Huffman, A.C., Jr., 1988, Revisions in nomenclature of the middle Jurassic Wanakah Formation, northwestern New Mexico and northeastern Arizona: U.S. Geological Survey Bulletin 1633–A, p. 1–12.
- Condon, S.M., and Peterson, F., 1986, Stratigraphy of middle and upper Jurassic rocks of the San Juan Basin—Historical perspectives, current ideas and remaining problems: American Association of Petroleum Geologists, Studies in Geology, no. 22, p. 7–26.
- Dane, C.H., Cobban, W.A., and Kauffman, E.G., 1966, Stratigraphy and regional relationships of a reference section for the Juana Lopez Member, Mancos Shale, in the San Juan Basin, New Mexico: U.S. Geological Survey Bulletin 1224–H, p. 1–15.
- Dethier, D.P., 1999, Quaternary evolution of the Rio Grande near Cochiti Lake, northern Santo Domingo basin, New Mexico: New Mexico Geological Society, 50th Field Conference, Albuquerque Geology, p. 371–378.
- Dethier, D.P., and McCoy, W.D., 1993, Aminostratigraphic relations and age of Quaternary deposits, northern Española basin, New Mexico: Quaternary Research, v. 39, p. 222–230.
- Disbrow, A.E., and Stoll, W.C., 1957, Geology of the Cerrillos area, Santa Fe County, New Mexico: New Mexico Bureau of Mines and Mineral Resources Bulletin 48, 73 p., 1:31,680-scale map.
- Erskine, D.W., and Smith, G.A., 1993, Compositional characterization of volcanic products from a primarily sedimentary record—The Oligocene Espinazo Formation, north-central New Mexico: Geological Society of America Bulletin, v. 105, p. 1214–1222.
- Gile, L.H., Peterson, F.F., and Grossman, R.B., 1966, Morphological and genetic sequences of carbonate accumulation in desert soils: Soil Science, v. 101, p. 347–360.
- Guthrie, R.L., and Witty, J.E., 1982, New designations for soil horizons and layers and the new Soil Survey Manual: Soil Science Society of America Journal, v. 46, p. 443–444.
- Hansen, W.R., 1991, Suggestions to authors of the reports of the United States Geological Survey, Seventh Edition: Washington, D.C., U.S. Government Printing Office, 289 p.
- Izett, G.A., and Obradovich, J.D., 1994,  $^{40}\text{Ar}/^{39}\text{Ar}$  age constraints of the Jaramillo normal subchron and the Matuyama-Brunhes geomagnetic boundary: Journal of Geophysical Research, v. 99, p. 2925–2934.
- Kelley, V.C., 1978, Geology of the Española Basin, New Mexico: New Mexico Bureau of Mines and Mineral Resources Geologic Map 48, scale 1:125,000.
- Kirkland, D.W., Denison, R.E., and Evans, R., 1995, Middle Jurassic Todilto Formation of northern New Mexico and southwestern Colorado—Marine or non-marine: New Mexico Bureau of Mines and Mineral Resources Bulletin 147, 37 p.
- Landis, E.R., and Dane, C.H., 1967, Geologic map of the Tierra Amarilla quadrangle, Rio Arriba County, New Mexico: New Mexico Bureau of Mines and Mineral Resources Geologic Map 19, scale 1:62,500.
- Landis, E.R., Dane, C.H., and Cobban, W.A., 1973, Stratigraphic terminology of the Dakota Sandstone and Mancos Shale, west-central New Mexico: U.S. Geological Survey Bulletin 1372–J, 44 p.
- Le Bas, M.J., Le Maitre, R.W., Streckeisen, A., and Zanettin, B., 1986, A chemical classification of volcanic rocks based on the total alkali-silica



- diagram: *Journal of Petrology*, v. 27, p. 745–750.
- Leckie, R.M., Kirkland, J.I., and Elder, W.P., 1997, Stratigraphic framework and correlation of a principal reference section of the Mancos Shale (Upper Cretaceous), Mesa Verde, Colorado: *New Mexico Geological Society, 48th Field Conference “Four Corners” Guidebook*, p. 163–216.
- Le Maitre, R.W., ed., 1989, *A classification of igneous rocks and glossary of terms*: Oxford, Blackwell Scientific Publications, 193 p.
- Lourens, L.J., Hilgen, F.J., Raffi, I., and Vergnaud-Grazzini, C., 1996, Early Pleistocene chronology of the Vrica section [Calabria, Italy]: *Paleoceanography*, v. 11, p. 797–812.
- Lucas, S.G., and Anderson, O.J., 1997, The Jurassic San Rafael Group, Four Corners region: *New Mexico Geological Society, 48th Field Conference “Four Corners” Guidebook*, p. 115–132.
- Lucas, S.G., Anderson, O.J., and Pigman, C., 1995, Jurassic stratigraphy in the Hagan basin, north-central New Mexico: *New Mexico Geological Society, 46th Field Conference “Santa Fe Region” Guidebook*, p. 247–256.
- Lucas, S.G., Cather, S.M., Abbott, J.C., and Williamson, T.E., 1997, Stratigraphy and tectonic implications of Paleogene strata in the Laramide Galisteo Basin, north-central New Mexico: *New Mexico Geology*, v. 19, p. 89–95.
- Machette, M.N., Long, Thomas, and Bachman, G.O., 1997, Laboratory data for calcic soils in central New Mexico—Background information for mapping Quaternary deposits in the Albuquerque basin: *U.S. Geological Survey Open-File Report 96-722*, 60 p.
- Maynard, S.R., 1995, Gold mineralization associated with mid-Tertiary magmatism and tectonism, Ortiz Mountains, Santa Fe County, New Mexico: *New Mexico Geological Society Guidebook, 46th Field Conference, Geology of the Santa Fe region*, p. 161–166.
- Molenaar, C.M., and Baird, J.K., 1992, Regional stratigraphic cross-sections of Upper Cretaceous rocks across the San Juan Basin, northwestern New Mexico and southwestern Colorado: *U.S. Geological Survey Open-File Report 92-257*, 3 sheets.
- Munsell Color, 1973, *Munsell soil color charts*: Baltimore, Md., Kollmorgen Corp., Macbeth Division.
- O’Sullivan, R.B., and Pierce, F.W., 1983, Stratigraphic diagram of Middle Jurassic San Rafael Group and associated formations from the San Rafael Swell to Bluff in southeast Utah: *U.S. Geological Survey Oil and Gas Investigations Chart OC-119*, 1 sheet.
- Owen, D.E., Walters, L.J., Jr., and Beck, R.G., 1984, The Jackpile Sandstone Member of the Morrison Formation in west-central New Mexico—A formal definition: *New Mexico Geology*, v. 6., p. 45–52.
- Peery, R.L., and Pearson, J.W., 1994, Hydrogeology and water-resource assessment, proposed La Bajada subdivision, Santa Fe County, NM: John Shomaker & Associates consultant report, 33 p. plus maps and tables.
- Reneau, S.L., Gardner, J.N., and Forman, S.L., 1996, New evidence for the age of the youngest eruption in the Valles caldera, New Mexico: *Geology*, v. 24, p. 7–10.
- Richmond, G.M., and Fullerton, D.S., 1986, Introduction to Quaternary glaciations in the United States of America, *in* Sibrava, V., Bowen, D.Q., and Richmond, G.M., eds., *Quaternary glaciations in the northern hemisphere: Quaternary Science Reviews*, v. 5, p. 3–10.
- Santos, E.S., 1975, Lithology and uranium potential of Jurassic formations in the San Ysidro–Cuba and Majors Ranch areas, northwestern New Mexico: *U.S. Geological Survey Bulletin 1329*, 22 p.
- Sauer, R.R., 1999, Petrochemistry and geochronology of plutons relative to tectonics in the San Pedro–Ortiz porphyry belt, New Mexico: *Boulder, Colo., University of Colorado M.S. thesis*, 115 p.
- Shroba, R.R., and Thompson, R.A., 1998, Eolian origin of sandy mantles on gently-sloping basaltic lava flows in the Pliocene Cerros del Rio volcanic field near Santa Fe, New Mexico—Preliminary findings [abs.], *in* Slate, J.L., ed., *U.S. Geological Survey Middle Rio Grande Basin Study—Proceedings of the second annual workshop, February 10–11, 1998: U.S. Geological Survey Open-File Report 98-337*, p. 24–25.
- Smith, G.A., and Kuhle, A.J., 1998, Geologic map of the Santo Domingo Pueblo and Santo Domingo Pueblo SW quadrangles, Sandoval County, New Mexico: *New Mexico Bureau of Mines and Mineral Resources Open-file Digital Map OF-DM-15 and OF-DM-26*, 1 sheet and text, scale 1:24,000.
- Soil Survey Staff, 1975, *Soil taxonomy: U.S. Department of Agriculture Handbook 436*, 754 p.
- Spiegel, Z., and Baldwin, B., 1963, *Geology and water resources of the Santa Fe area, New Mexico: U.S. Geological Survey Water-Supply Paper 1525*, 258 p.
- Stearns, C.E., 1953a, Tertiary geology of the Galisteo-Tonque area, New Mexico: *Geological Society of America Bulletin*, v. 64, p. 459–508.
- 1953b, Early Tertiary volcanism in the Galisteo-Tonque area, north-central New Mexico: *American Journal of Science*, v. 251, p. 415–452.
- Sun, M., and Baldwin, B., 1958, Volcanic rocks of the Cienega area, Santa Fe County, New Mexico: *New Mexico Bureau of Mines and Mineral Resources Bulletin 54*, 80 p., 1:15,840-scale map.

- U.S. Geological Survey, Sander Geophysics, Ltd., and Geotrex-Dighem, 1999, Digital aeromagnetic data from the Sandoval-Santa Fe, Belen, and Cochiti airborne surveys, covering areas in Rio Arriba, Sandoval, Santa Fe, Socorro, and Valencia Counties, New Mexico: U.S. Geological Survey Open-File Report 99-404, 1 CD-ROM.
- Varnes, D.J., 1978, Slope movement types and process, *in* Schuster, R.L., and Krizek, R.J., eds., *Landslides, analysis, and control*: National Academy of Sciences, Transportation Research Board Special Report 176, p. 11-33.
- Woldegabriel, G., Laughlin, A.W., Dethier, D.P., and Heizler, M., 1996, Temporal and geochemical trends of lavas in White Rock Canyon and the Pajarito Plateau, Jemez Volcanic Field, New Mexico, USA: New Mexico Geological Society Guidebook, 47th Field Conference "Jemez Mountains Region", p. 251-261.
- Zimmerman, C., and Kudo, A.M., 1979, Geology and petrology of Tetilla Peak: New Mexico Geological Society Guidebook, 30th Field Conference "Santa Fe Country", p. 253-256.

**Table 3.** Major-element chemistry of Tertiary igneous rocks, Tetilla Peak and adjoining 7.5-minute quadrangles  
[\* indicates greater age uncertainty or disagreement with stratigraphic relationships]

| <u>Basalt of Caja del Rio (Tbr)</u> |                               |                           |                          |                               |                               |                               |                 |                                   |
|-------------------------------------|-------------------------------|---------------------------|--------------------------|-------------------------------|-------------------------------|-------------------------------|-----------------|-----------------------------------|
| Map unit<br>Rock name               | Tbr<br>Transitional<br>basalt | Tbr<br>Alkaline<br>basalt | Tbr—dike<br>Trachybasalt | Tbr<br>Transitional<br>basalt | Tbr<br>Transitional<br>basalt | Tbr<br>Transitional<br>basalt | Tbr<br>Basanite | Tbr<br>Basaltic<br>trachyandesite |
| Field No.<br>Map No.                | 96DTP24<br>D24                | 96DTP11<br>D11            | 96DTP12<br>D12           | 96DTP09<br>D09                | 96DTP08<br>D08                | 96DTP07<br>D07                | 96DTP05<br>D05  | 79ZTP04<br>Z04                    |
| SiO <sub>2</sub> %                  | 48.7                          | 48.4                      | 49.3                     | 48.8                          | 48.9                          | 48.7                          | 47.2            | 52.1                              |
| Al <sub>2</sub> O <sub>3</sub> %    | 17.3                          | 16.1                      | 17.3                     | 16.5                          | 16.4                          | 16.1                          | 15.9            | 15.1                              |
| FeTO <sub>3</sub> %                 | 10.6                          | 10.9                      | 11.3                     | 11.3                          | 11.4                          | 11.3                          | 10.1            | 9.21                              |
| MgO %                               | 5.95                          | 7.19                      | 5.30                     | 6.57                          | 7.24                          | 7.58                          | 7.41            | 7.14                              |
| CaO %                               | 9.66                          | 10.26                     | 9.00                     | 9.17                          | 8.85                          | 9.02                          | 9.39            | 8.45                              |
| Na <sub>2</sub> O %                 | 3.63                          | 3.60                      | 4.00                     | 3.79                          | 3.69                          | 3.69                          | 4.28            | 3.86                              |
| K <sub>2</sub> O %                  | 1.44                          | 1.02                      | 1.16                     | 1.06                          | 1.03                          | 1.05                          | 1.99            | 2.11                              |
| TiO <sub>2</sub> %                  | 1.58                          | 1.47                      | 1.63                     | 1.59                          | 1.54                          | 1.48                          | 1.72            | 1.44                              |
| P <sub>2</sub> O <sub>5</sub> %     | 0.83                          | 0.58                      | 0.59                     | 0.58                          | 0.57                          | 0.59                          | 1.20            | 0.89                              |
| MnO %                               | 0.17                          | 0.16                      | 0.16                     | 0.16                          | 0.16                          | 0.16                          | 0.17            | 0.15                              |
| LOI-925°C                           | 0.24                          | 1.50                      | 0.80                     | -0.09                         | -0.32                         | -0.10                         | 0.19            | 0.61                              |
| Total                               | 99.84                         | 99.67                     | 99.69                    | 99.49                         | 99.79                         | 99.56                         | 99.34           | 100.54                            |
| Total alkalis %                     | 5.06                          | 4.63                      | 5.16                     | 4.85                          | 4.71                          | 4.74                          | 6.27            | 5.98                              |
| Na <sub>2</sub> O-2<br>ne           | 1.63                          | 1.60                      | 2.00                     | 1.79                          | 1.69                          | 1.69                          | 2.28            | 1.86                              |
| hy                                  | 0.82                          | 2.12                      | 0.37                     | 0.34                          | 0.00                          | 0.48                          | 8.10            | 0.00                              |
| q                                   | 0.00                          | 0.00                      | 0.00                     | 0.00                          | 1.28                          | 0.00                          | 0.00            | 4.61                              |
| pl An %                             | 0.00                          | 0.00                      | 0.00                     | 0.00                          | 0.00                          | 0.00                          | 0.00            | 0.00                              |
|                                     | 47.6                          | 48.3                      | 43.9                     | 44.2                          | 44.5                          | 44.4                          | 45.8            | 35.0                              |
| Age (Ma)                            | 2.44                          |                           | 2.42                     | *2.03                         |                               |                               | 2.35            |                                   |
| Uncertainty                         | 0.06                          |                           | 0.03                     | 0.35                          |                               |                               | 0.06            |                                   |
| IUGS name                           | Hawaiite                      | Akaline<br>basalt         | Hawaiite                 | Alkaline<br>basalt            | Alkaline<br>basalt            | Alkaline<br>basalt            | Basanite        | Basaltic<br>trachyandesite        |
| Field name                          |                               |                           |                          |                               |                               |                               |                 |                                   |

**Table 3.** Major-element chemistry of Tertiary igneous rocks, Tetilla Peak and adjoining 7.5-minute quadrangles—Continued

| Map unit<br>Rock name<br>Field No.<br>Map No. | Dacite of Tetilla Peak (Tdt)    |                                 | Andesite of Tetilla Peak (Tat)    |                                 |                                 |                                 | Basalt of La Bajada (Tbb)             |                                       |                                       |
|---|---------------------------------|---------------------------------|-----------------------------------|---------------------------------|---------------------------------|---------------------------------|---------------------------------------|---------------------------------------|---------------------------------------|
|   | Tdt<br>Dacite<br>96TTP01<br>T01 | Tdt<br>Dacite<br>79ZTP10<br>Z10 | Tat<br>Andesite<br>96DTP10<br>D10 | Tat<br>Latite<br>96DTP34<br>D34 | Tat<br>Latite<br>79ZTP05<br>Z05 | Tat<br>Latite<br>96DTP06<br>D06 | Tbb<br>Trachybasalt<br>96DTP03<br>D03 | Tbb<br>Trachybasalt<br>96DTP02<br>D02 | Tbb<br>Trachybasalt<br>96DTP19<br>D19 |
| SiO <sub>2</sub> %                            | 63.4                            | 64.0                            | 62.7                              | 61.2                            | 61.1                            | 56.5                            | 48.0                                  | 48.9                                  |                                       |
| Al <sub>2</sub> O <sub>3</sub> %              | 15.2                            | 15.6                            | 15.8                              | 15.7                            | 15.6                            | 16.7                            | 15.9                                  | 15.8                                  |                                       |
| FeTO <sub>3</sub> %                           | 4.63                            | 3.94                            | 5.05                              | 5.39                            | 5.61                            | 6.96                            | 10.49                                 | 9.71                                  |                                       |
| MgO %   | 2.74                            | 2.48                            | 2.77                              | 3.33                            | 3.21                            | 3.49                            | 7.09                                  | 7.57                                  |                                       |
| CaO %   | 5.22                            | 4.39                            | 4.82                              | 5.50                            | 5.61                            | 6.69                            | 9.39                                  | 9.53                                  |                                       |
| Na <sub>2</sub> O %                           | 4.08                            | 4.16                            | 3.90                              | 4.11                            | 4.38                            | 4.32                            | 3.78                                  | 2.97                                  |                                       |
| K <sub>2</sub> O %                            | 2.96                            | 3.13                            | 2.94                              | 2.77                            | 2.47                            | 2.39                            | 1.83                                  | 2.03                                  |                                       |
| TiO <sub>2</sub> %                            | 0.63                            | 0.65                            | 0.68                              | 0.73                            | 0.76                            | 1.10                            | 1.78                                  | 1.56                                  |                                       |
| P <sub>2</sub> O <sub>5</sub> %               | 0.52                            | 0.45                            | 0.52                              | 0.69                            | 0.66                            | 1.06                            | 1.05                                  | 1.01                                  |                                       |
| MnO %   | 0.09                            | 0.09                            | 0.09                              | 0.10                            | 0.10                            | 0.11                            | 0.17                                  | 0.17                                  |                                       |
| LOI-925°C                                     | 1.90                            | 1.51                            | 1.85                              | 0.86                            | 0.46                            | 1.11                            | 1.70                                  | 2.64                                  |                                       |
| Total   | 99.45                           | 98.92                           | 99.30                             | 99.49                           | 99.48                           | 99.29                           | 99.49                                 | 99.31                                 |                                       |
| Total alkalis %                               | 7.04                            | 7.29                            | 6.84                              | 6.88                            | 6.85                            | 6.71                            | 5.61                                  | 5.00                                  |                                       |
| Na <sub>2</sub> O-2                           | 2.08                            | 2.16                            | 1.90                              | 2.11                            | 2.38                            | 2.32                            | 1.78                                  | 0.97                                  |                                       |
| ne  | 0.00                            | 0.00                            | 0.00                              | 0.00                            | 0.00                            | 0.00                            | 3.63                                  | 0.00                                  |                                       |
| hy  | 5.23                            | 4.96                            | 7.48                              | 8.20                            | 7.59                            | 9.41                            | 0.00                                  | 3.83                                  |                                       |
| q   | 15.8                            | 17.0                            | 15.9                              | 12.3                            | 11.9                            | 5.80                            | 0.00                                  | 0.00                                  |                                       |
| pl An %                                       | 29.4                            | 29.5                            | 33.9                              | 32.0                            | 29.5                            | 34.3                            | 45.5                                  | 48.7                                  |                                       |
| Age (Ma)                                      | *2.78                           |                                 | *3.04                             |                                 |                                 |                                 |                                       |                                       | 2.62                                  |
| Uncertainty                                   | 0.27                            |                                 | 0.21                              |                                 |                                 |                                 |                                       |                                       | 0.14                                  |
| IUGS name                                     | Dacite                          | Trachyte                        | Andesite                          | Latite                          | Latite                          | Latite                          | Potassic<br>trachybasalt              | Potassic<br>trachybasalt              |                                       |
| Field name                                    |                                 |                                 |                                   |                                 |                                 |                                 |                                       |                                       |                                       |

**Table 3.** Major-element chemistry of Tertiary igneous rocks, Tetilla Peak and adjoining 7.5-minute quadrangles—Continued

| Map unit<br>Rock name            | Basalt of<br>La Bajada (Tbb) |   | Basalt of Tsinat Mesa (Tbs) |                          |                                 |  |                               |                          |                  |
|----------------------------------|------------------------------|---|-----------------------------|--------------------------|---------------------------------|--|-------------------------------|--------------------------|------------------|
|                                  | Tbb<br>Basalt                | Tbs—dike<br>Basaltic<br>trachy-<br>andesite | Tbs<br>Trachy-<br>basalt    | Tbs<br>Trachy-<br>basalt | Tbs<br>Trachy-<br>basalt        | Tbs<br>Basaltic<br>trachy-<br>andesite | Tbs<br>Trachy-<br>basalt      | Tbs<br>Trachy-<br>basalt | Tbs<br>Basalt    |
| Field No.<br>Map No.             | SMRGB-1<br>M01 <sup>1</sup>  | 96DTP01<br>D01                              | 96DTP04<br>D04              | 58BTP85<br>B85           | 96TTH02a<br>TTH02a <sup>1</sup> | 96TTH02b<br>TTH02b <sup>1</sup>        | 96TTH01<br>TTH01 <sup>1</sup> | 97DTP99<br>D99           | 97DTP98A<br>D98A |
| SiO <sub>2</sub> %               | 49.0                         | 52.7  | 50.9                        | 51.4                     | 51.6                            | 52.3                                   | 47.2                          | 47.4                     | 47.8             |
| Al <sub>2</sub> O <sub>3</sub> % | 16.9                         | 15.5  | 15.7                        | 14.9                     | 15.4                            | 15.6                                   | 15.6                          | 15.6                     | 14.9             |
| FeTO <sub>3</sub> %              | 11.0                         | 8.43  | 9.16                        | 9.54                     | 8.96                            | 8.62                                   | 11.2                          | 10.1                     | 11.1             |
| MgO %                            | 5.99                         | 6.28  | 7.01                        | 6.54                     | 7.22                            | 6.51                                   | 7.47                          | 7.94                     | 7.69             |
| CaO %                            | 10.0                         | 7.69  | 7.92                        | 9.42                     | 7.59                            | 7.45                                   | 8.98                          | 9.43                     | 9.58             |
| Na <sub>2</sub> O %              | 3.10                         | 4.04  | 3.99                        | 3.33                     | 3.55                            | 4.01                                   | 3.96                          | 4.22                     | 3.23             |
| K <sub>2</sub> O %               | 1.20                         | 2.33  | 2.21                        | 2.10                     | 2.18                            | 2.35                                   | 1.83                          | 1.43                     | 1.68             |
| TiO <sub>2</sub> %               | 1.60                         | 1.45  | 1.53                        | 1.54                     | 1.44                            | 1.49                                   | 1.88                          | 1.61                     | 1.76             |
| P <sub>2</sub> O <sub>5</sub> %  | 0.60                         | 0.79  | 0.91                        | 1.08                     | 0.83                            | 0.82                                   | 0.99                          | 1.14                     | 1.12             |
| MnO %                            | 0.18                         | 0.14  | 0.15                        | 0.15                     | 0.15                            | 0.14                                   | 0.18                          | 0.17                     | 0.19             |
| LOI-925°C                        | 1.42                         | 0.50  | 1.44                        | 2.70                     | 1.64                            | 0.00                                   | -0.30                         | 0.31                     | 1.59             |
| Total                            | 99.67                        | 99.44                                       | 99.44                       | 100.07                   | 98.87                           | 99.20                                  | 99.21                         | 99.02                    | 99.10            |
| Total alkalis %                  | 4.29                         | 6.38  | 6.20                        | 5.43                     | 5.73                            | 6.36                                   | 5.79                          | 5.65                     | 4.91             |
| Na <sub>2</sub> O-2<br>ne        | 1.10                         | 2.04  | 1.99                        | 1.33                     | 1.55                            | 2.01                                   | 1.96                          | 2.22                     | 1.23             |
| hy                               | 0.00                         | 0.00  | 0.00                        | 0.00                     | 0.00                            | 0.00                                   | 5.46                          | 7.25                     | 1.78             |
| q                                | 3.61                         | 7.39  | 0.00                        | 10.46                    | 12.13                           | 6.91                                   | 0.00                          | 0.00                     | 0.00             |
| pl An %                          | 0.00                         | 0.00  | 0.00                        | 0.00                     | 0.00                            | 0.00                                   | 0.00                          | 0.00                     | 0.00             |
| Age (Ma)                         | ~2.7 Ma                      | 2.68  |                             |                          |                                 |  |                               |                          |                  |
| Uncertainty                      |                              | 0.03  |                             |                          |                                 |  |                               |                          |                  |
| IUGS name                        | Subalkaline<br>basalt        | Shoshonite                                  | Potassic<br>trachybasalt    | Potassic<br>trachybasalt | Potassic<br>trachybasalt        | Shoshonite                             | Hawaiite                      | Hawaiite                 | Hawaiite         |
| Field name                       | Olivine<br>basalt            |   |                             |                          |                                 |  |                               |                          |                  |

<sup>1</sup>Map No. M01 is located on adjoining Santo Domingo Pueblo 7.5' quadrangle; map Nos. TTH02a, TTH02b, and TTH01 are located on adjoining Turquoise Hill 7.5' quadrangle.

**Table 3.** Major-element chemistry of Tertiary igneous rocks, Tetilla Peak and adjoining 7.5-minute quadrangles—Continued

| Map unit<br>Rock name            | Basalt of Mesita de Juana (Tbj) |                          |                 | Cieneguilla Basanite (Tc) |                     |                |                     |                  |                |
|----------------------------------|---------------------------------|--------------------------|-----------------|---------------------------|---------------------|----------------|---------------------|------------------|----------------|
|                                  | Tbj—dike<br>Trachy-<br>basalt   | Tbj<br>Trachy-<br>basalt | Tbj<br>Basanite | Tc<br>Basalt              | Tc—dike<br>Basanite | Tc<br>Basanite | Tc—dike<br>Basanite | Tc<br>Basanite   | Tc<br>Basanite |
| Field No.<br>Map No.             | 96DTP15<br>D15                  | 96DTP14<br>D14           | 96DTP13<br>D13  | 58BTP142<br>B142          | 58BTP49<br>B49      | 96DTP30<br>D30 | 58BTP48<br>B48      | 79STPA71<br>SA71 | 97DTP91<br>D91 |
| SiO <sub>2</sub> %               | 47.3                            | 47.5                     | 44.8            | 47.6                      | 43.1                | 42.9           | 42.0                | 42.0             | 42.7           |
| Al <sub>2</sub> O <sub>3</sub> % | 15.6                            | 15.6                     | 15.4            | 14.6                      |                     | 12.2           |                     | 11.3             | 11.9           |
| FeTO <sub>3</sub> %              | 11.2                            | 11.4                     | 11.5            | 14.0                      |                     | 14.0           |                     | 11.9             | 13.1           |
| MgO %                            | 8.65                            | 8.67                     | 8.45            | 9.13                      |                     | 12.3           |                     | 15.4             | 13.0           |
| CaO %                            | 9.21                            | 9.15                     | 10.27           | 9.81                      |                     | 11.1           |                     | 12.8             | 11.5           |
| Na <sub>2</sub> O %              | 3.73                            | 3.66                     | 4.05            | 2.59                      |                     | 2.79           |                     | 3.05             | 2.86           |
| K <sub>2</sub> O %               | 1.33                            | 1.37                     | 1.63            | 0.89                      |                     | 0.63           |                     | 0.80             | 1.15           |
| TiO <sub>2</sub> %               | 1.74                            | 1.75                     | 1.87            | 1.69                      |                     | 2.31           |                     | 1.86             | 2.06           |
| P <sub>2</sub> O <sub>5</sub> %  | 0.74                            | 0.71                     | 1.28            | 0.29                      |                     | 0.78           |                     | 1.00             | 0.87           |
| MnO %                            | 0.17                            | 0.17                     | 0.18            | 0.20                      |                     | 0.20           |                     | 0.00             | 0.20           |
| LOI-925°C                        | -0.13                           | -0.11                    | -0.38           | 3.74                      |                     | 1.04           |                     | -1.19            | 0.99           |
| Total                            | 99.68                           | 99.92                    | 99.34           | 100.76                    |                     | 99.19          |                     | 100.00           | 99.29          |
| Total alkalis %                  | 5.06                            | 5.03                     | 5.68            | 3.48                      |                     | 3.42           |                     | 3.85             | 4.00           |
| Na <sub>2</sub> O-2<br>ne        | 1.73                            | 1.66                     | 2.05            | 0.59                      |                     | 0.79           |                     | 1.05             | 0.86           |
| hy                               | 3.94                            | 3.61                     | 10.83           | 0.00                      |                     | 8.03           |                     | 13.84            | 11.52          |
| q                                | 0.00                            | 0.00                     | 0.00            | 5.51                      |                     | 0.00           |                     | 0.00             | 0.00           |
| pl An %                          | 0.00                            | 0.00                     | 0.00            | 0.00                      |                     | 0.00           |                     | 0.00             | 0.00           |
|                                  | 47.3                            | 47.4                     | 56.3            | 54.0                      |                     | 68.8           |                     | 100              | 85.8           |
| Age (Ma)                         | 2.69                            |                          | 2.66            |                           |                     |                |                     |                  |                |
| Uncertainty                      | 0.08                            |                          | 0.08            |                           |                     |                |                     |                  |                |
| IUGS name                        | Hawaiite                        | Hawaiite                 | Basanite        | Subalkaline<br>basalt     | Basanite            | Basanite       | Basanite            | Basanite         | Basanite       |
| Field name                       |                                 |                          |                 | Olivine<br>basalt         |                     |                |                     |                  |                |

**Table 3.** Major-element chemistry of Tertiary igneous rocks, Tetilla Peak and adjoining 7.5-minute quadrangles—Continued

| Map unit<br>Rock name            | Cieneguilla Basanite (Tc) |                     |                     |                               |                               |                               | Cerrillos intrusion           |                                |
|----------------------------------|---------------------------|---------------------|---------------------|-------------------------------|-------------------------------|-------------------------------|-------------------------------|--------------------------------|
|                                  | Tc<br>Basanite            | Tc—dike<br>Basanite | Tc—dike<br>Basanite | Tc<br>Nephelinite             | Tc<br>Nephelinite             | Tc—dike<br>Nephelinite        | Tc—dike<br>Nephelinite        | Tmh<br>Hornblende<br>monzonite |
| Field No.<br>Map No.             | 97DTP88<br>D88            | SM96-49<br>M49      | 97DTP101<br>D101    | 53STH27<br>STH27 <sup>2</sup> | 97DTH13<br>DTH13 <sup>2</sup> | 97DMA01<br>DMA01 <sup>2</sup> | 58BTH73<br>BTH73 <sup>2</sup> | 97DPR01<br>DPR01 <sup>2</sup>  |
| SiO <sub>2</sub> %               | 41.9                      | 40.6                | 38.2                | 40.9                          | 40.3                          | 40.4                          | 39.0                          | 58.1                           |
| Al <sub>2</sub> O <sub>3</sub> % | 12.3                      | 11.4                | 10.5                | 11.9                          | 11.4                          | 11.0                          |                               | 17.7                           |
| FeTO <sub>3</sub> %              | 13.4                      | 12.9                | 12.4                | 11.9                          | 11.8                          | 11.6                          |                               | 6.61                           |
| MgO %                            | 13.3                      | 14.9                | 15.3                | 14.5                          | 14.0                          | 15.0                          |                               | 2.61                           |
| CaO %                            | 11.7                      | 13.4                | 16.7                | 13.5                          | 13.9                          | 13.7                          |                               | 6.11                           |
| Na <sub>2</sub> O %              | 2.90                      | 1.99                | 1.30                | 3.54                          | 3.59                          | 2.71                          |                               | 4.22                           |
| K <sub>2</sub> O %               | 0.73                      | 0.75                | 0.66                | 0.74                          | 0.70                          | 1.28                          |                               | 2.27                           |
| TiO <sub>2</sub> %               | 2.22                      | 2.12                | 2.03                | 2.71                          | 2.29                          | 1.76                          |                               | 0.70                           |
| P <sub>2</sub> O <sub>5</sub> %  | 0.76                      | 0.94                | 1.39                | 0.69                          | 1.09                          | 1.12                          |                               | 0.27                           |
| MnO %                            | 0.19                      | 0.20                | 0.22                | 0.08                          | 0.20                          | 0.19                          |                               | 0.16                           |
| LOI-925°C                        | 1.25                      | 2.41                | 2.83                | 1.71                          | 1.30                          | 7.13                          |                               | 2.14                           |
| Total                            | 99.36                     | 99.23               | 98.66               | 100.48                        | 99.14                         | 98.75                         |                               | 98.77                          |
| Total alkalis %                  | 3.63                      | 2.74                | 1.96                | 4.28                          | 4.29                          | 3.99                          |                               | 6.49                           |
| Na <sub>2</sub> O-2<br>ne        | 0.90                      | -0.01               | -0.70               | 1.54                          | 1.59                          | 0.71                          |                               | 2.22                           |
| hy                               | 12.12                     | 8.89                | 5.77                | 16.27                         | 16.22                         | 11.50                         |                               |                                |
| q                                | 0.00                      | 0.00                | 0.00                | 0.00                          | 0.00                          | 0.00                          |                               |                                |
| pl An %                          | 91.0                      | 100                 | 100                 | 100                           | 100                           | 100                           |                               | 38.8                           |
| Age (Ma)<br>Uncertainty          |                           |                     |                     |                               |                               |                               |                               |                                |
| IUGS name<br>Field name          | Basanite                  | Basanite            | Basanite            | Nephelinite<br>Limburgite     | Nephelinite                   | Nephelinite                   | Nephelinite                   |                                |

<sup>2</sup>Map Nos. STH27, DTH13, and BTH73 are located on adjoining Turquoise Hill 7.5' quadrangle; map No. DMA01 is located on adjoining Madrid 7.5' quadrangle; map No. DPR01 is located on adjoining Picture Rock 7.5' quadrangle.

**Table 3.** Major-element chemistry of Tertiary igneous rocks, Tetilla Peak and adjoining 7.5-minute quadrangles—Continued

| Map unit<br>Rock name            | Espinaso Formation (Te)   |                             |                               | Cerrillos intrusion (Tmi) |                  |                               |                               |                  |
|----------------------------------|---------------------------|-----------------------------|-------------------------------|---------------------------|------------------|-------------------------------|-------------------------------|------------------|
|                                  | Te<br>Trachy-<br>andesite | Te<br>Trachy-<br>dacite     | Te<br>Latite                  | Tmi<br>Monzonite          | Tmi<br>Monzonite | Tmi<br>Monzonite              | Tmi<br>Monzonite              | Tmi<br>Monzonite |
| Field No.<br>Map No.             | 58BTP162<br>B162          | 58BTH92<br>B92 <sup>3</sup> | 58BTH72B<br>B72B <sup>3</sup> | 58BTP84<br>B84            | 97DTP96<br>D96   | 97DTH12<br>DTH12 <sup>3</sup> | 97DTH11<br>DTH11 <sup>3</sup> | 97DTP97<br>D97   |
| SiO <sub>2</sub> %               | 60.0                      | 66.2                        | 56.2                          | 61.0                      | 53.4             | 53.4                          | 53.7                          | 62.3             |
| Al <sub>2</sub> O <sub>3</sub> % | 17.8                      | 16.6                        | 17.5                          | 16.4                      | 17.9             | 18.2                          | 18.3                          | 17.5             |
| FeTO <sub>3</sub> %              | 6.25                      | 4.07                        | 8.98                          | 6.26                      | 8.46             | 7.92                          | 7.56                          | 4.41             |
| MgO %                            | 1.86                      | 0.48                        | 1.82                          | 1.26                      | 3.08             | 2.86                          | 2.66                          | 1.56             |
| CaO %                            | 6.45                      | 3.25                        | 6.63                          | 5.76                      | 7.32             | 6.93                          | 6.81                          | 3.99             |
| Na <sub>2</sub> O %              | 4.02                      | 4.72                        | 4.15                          | 3.94                      | 3.95             | 4.18                          | 4.18                          | 4.46             |
| K <sub>2</sub> O %               | 2.25                      | 3.68                        | 3.85                          | 3.92                      | 3.32             | 3.95                          | 4.03                          | 3.85             |
| TiO <sub>2</sub> %               | 0.64                      | 0.55                        | 0.86                          | 0.67                      | 0.86             | 0.85                          | 0.86                          | 0.48             |
| P <sub>2</sub> O <sub>5</sub> %  | 0.35                      | 0.15                        | 0.53                          | 0.28                      | 0.54             | 0.58                          | 0.53                          | 0.24             |
| MnO %                            | 0.01                      | 0.07                        | 0.08                          | 0.16                      | 0.19             | 0.21                          | 0.20                          | 0.13             |
| LOI-925°C                        | 2.65                      | 1.53                        | 1.91                          | 1.54                      | 0.18             | 0.22                          | 0.22                          | 1.21             |
| Total                            | 99.60                     | 99.74                       | 100.60                        | 99.72                     | 99.05            | 99.08                         | 98.80                         | 98.86            |
| Total alkalis %                  | 6.27                      | 8.40                        | 8.00                          | 7.86                      | 7.27             | 8.13                          | 8.22                          | 8.30             |
| Na <sub>2</sub> O-2<br>ne        | 2.02                      | 2.72                        | 2.15                          | 1.94                      | 1.95             | 2.18                          | 2.18                          | 2.46             |
| hy                               | 0.00                      | 0.00                        | 0.00                          | 0.00                      | 0.00             | 2.94                          | 2.52                          | 0.00             |
| q                                | 6.18                      | 1.21                        | 7.30                          | 2.64                      | 0.00             | 0.00                          | 0.00                          | 8.87             |
| pl An %                          | 12.0                      | 17.6                        | 0.9                           | 10.3                      | 0.00             | 0.00                          | 0.00                          | 9.23             |
|                                  | 41.2                      | 24.7                        | 33.7                          | 31.9                      | 39.0             | 39.1                          | 38.6                          | 30.3             |
| Age (Ma)<br>Uncertainty          |                           |                             |                               |                           |                  |                               |                               |                  |
| IUGS name<br>Field name          |                           |                             | Latite breccia<br>Andesite    |                           |                  |                               |                               |                  |

<sup>3</sup>Map Nos. B92, B72B, DTH12, and DTH11 are located on adjoining Turquoise Hill 7.5' quadrangle.



**Table 4.** Isotopic ages of Tertiary volcanic rocks, Tetilla Peak and adjoining Santo Domingo Pueblo  
7.5-minute quadrangles  
[<sup>40</sup>Ar/<sup>39</sup>Ar isotopic ages by W.C. McIntosh, New Mexico Geochronology Lab]

| Age <sup>1</sup>     | Uncertainty | Sample #  | Unit     | UTM-e (x) | UTM-n (y) |
|----------------------|-------------|-----------|----------|-----------|-----------|
| Tetilla Peak         |             |           |          |           |           |
| 2.42                 | 0.03        | 96DTP12   | Tbr      | 393583    | 3941401   |
| 2.03*                | 0.35        | 96DTP09   | Tbr      | 391719    | 3941367   |
| 2.35                 | 0.06        | 96DTP05   | Tbr      | 389500    | 3935867   |
| 2.44                 | 0.06        | 96DTP24   | Tbr      | 388458    | 3940795   |
| 2.78*                | 0.27        | 96TTP01   | Tdt      | 390483    | 3940961   |
| 3.04*                | 0.21        | 96DTP10   | Tat      | 391556    | 3941358   |
| 2.62                 | 0.14        | 96DTP19   | Tbb      | 388102    | 3940122   |
| 2.68                 | 0.03        | 96DTP01   | Tbs—dike | 398008    | 3942028   |
| 2.66                 | 0.08        | 96DTP13   | Tbj      | 391126    | 3931316   |
| 2.69                 | 0.08        | 96DTP15   | Tbj—dike | 393787    | 3932086   |
| 2.80                 | 0.10        | BachMen20 | Tbj      | 393184    | 3928949   |
| Santo Domingo Pueblo |             |           |          |           |           |
| 2.71                 | 0.04        | DN-96-15  | Tbp      | 381769    | 3938686   |

<sup>1</sup>Ages with \* are out of stratigraphic order with respect to field relations or other ages, and are therefore probably in error.